

## Non-invasive Investigations of Paintings by Portable Instrumentation: The MOLAB Experience

B. Brunetti<sup>1,2</sup> · C. Miliani<sup>1,2</sup> · F. Rosi<sup>2</sup> ·  
B. Doherty<sup>2</sup> · L. Monico<sup>2</sup> · A. Romani<sup>1,2</sup> ·  
A. Sgamellotti<sup>1,2</sup>

Received: 18 October 2015 / Accepted: 17 December 2015  
© Springer International Publishing Switzerland 2016

**Abstract** The in situ non invasive methods have experienced a significant development in the last decade because they meet specific needs of analytical chemistry in the field of cultural heritage where artworks are rarely moved from their locations, sampling is rarely permitted, and analytes are a wide range of inorganic, organic and organometallic substances in complex and precious matrices. MOLAB, a unique collection of integrated mobile instruments, has greatly contributed to demonstrate that it is now possible to obtain satisfactory results in the study of a variety of heritage objects without sampling or moving them to a laboratory. The current chapter describes an account of these results with particular attention to ancient, modern, and contemporary paintings. Several non-invasive methods by portable equipment, including XRF, mid- and near-FTIR, UV–Vis and Raman spectroscopy, as well as XRD, are discussed in detail along with their impact on our understanding of painting materials and execution techniques. Examples of successful applications are given, both for point analyses and hyperspectral imaging approaches. Lines for future perspectives are finally drawn.

**Keywords** X-ray fluorescence · Raman spectroscopy · FTIR · UV–Vis spectroscopy · Pigment · Binding media

---

✉ B. Brunetti  
bruno@dyn.unipg.it

<sup>1</sup> Centro di Eccellenza SMAArt (Scientific Methodologies Applied to Archaeology and Art), Università degli Studi di Perugia, Via Elce di Sotto 8, 06123 Perugia, Italy

<sup>2</sup> Istituto CNR di Scienze e Tecnologie Molecolari (CNR-ISTM), Via Elce di Sotto 8, 06123 Perugia, Italy

## 1 Introduction

In recent decades there has been a growing interest in the applications of analytical chemistry for the study of heritage materials. Through scientific examinations, satisfactory answers have been given to numerous problems of a multidisciplinary nature, such as the clarification of historical art and archaeological questions (i.e. execution techniques, attribution, dating, provenance), the assessment of the state of conservation of artefacts, the establishment of the best conditions to avoid or slow down alterations, as well as the monitoring of the behaviour of artwork materials during and after restoration [1, 2].

These studies were carried out in the past mostly by micro-destructive methods using minimal samples, taken from marginal areas of the artwork during restoration, in order to mitigate the visual impact of the operation. In other cases, the first relevant non-invasive analytical approaches were experimented by moving artifacts, such as manuscripts or small paintings, into a scientific laboratory, and exploiting bench-top instrumentation (e.g. micro-Raman spectrometers) [3, 4] or accelerators and large scale facility methods [5–8].

However, a large portion of historical patrimony consists in immovable objects that cannot be moved from their usual location (e.g. monuments, sculptures, buildings) and, even in the case of movable patrimony (including precious paintings, ceramics, gems, manuscripts, etc.), curators normally avoid moving artworks to a laboratory due to the risk to their integrity and high insurance costs. For such reasons, many efforts over the years have been oriented towards the design and set up of innovative mobile instruments with sensitivity and specificity comparable to their bench-top counterparts, achieving the best compromise between efficiency and portability in order to apply a method based on bringing the laboratory to the object and not vice versa.

Such an in situ, non-invasive approach, being able to get valuable information without altering or moving the object, registered an immediate success, leading to a rapid diffusion of the use of portable instrumentation that produced in recent years: (a) a significant change in diagnostic practices, (b) a net increase of scientific inputs in heritage studies and (c) a positive modification in the relationships between curators, conservators, and scientists, thus permitting a common language to be established and partnership strengthened.

After the first national Italian applications and the pioneering and successful MOLAB (mobile laboratory) experience of the European projects Eu-ARTECH (2004–2009) [9] and CHARISMA (2009–2014) [10], where a set of integrated portable instrumentations were offered to European users for in situ measurements, more and more mobile tools and facilities flourished in different countries that now permit users, through the national and European IPERION CH programmes [11], to exploit integrated portable instruments able to non-invasively obtain satisfying results in the study of a variety of heritage objects and relative inorganic and organic materials.

In this chapter, following a short general introduction on the limitations and advantages intrinsic to the use of compact portable instrumentation for analytical

applications, selected experimental results are presented, mostly obtained in recent works by MOLAB [12]. The aim is to show actual performances of the non-invasive approach in the study of atomic and molecular composition of artwork materials, with particular focus on pigments, colorants and binding media in ancient and modern paintings.

More recently, following the success of point analyses, innovative chemical imaging techniques at the macro scale have been also experimentally applied for in situ examination of paintings. Indications are given on perspectives for future developments along this direction.

## 2 Portable Spectroscopic Instrumentation: Benefits and Drawbacks

Passing from bench-top instrumentation to the compact and manageable equipment for in situ measurements some limitations may be incurred in term of performance, due to the miniaturization of optical and electronic components and constraints in the setup geometry. Nevertheless, the performance of portable spectroscopic instruments has greatly improved in the past decade, narrowing the gap between portable and bench-top instruments.

Relevant issues can arise regarding spectral interpretation due to the optical and matrix effects that are present each time a signal is recorded in backscattering, emission, or reflection mode from materials having a complex, heterogeneous, and often multi-layered character, as occurs in polychromies.

However, the use of a variety of equipment, a non-invasive approach, and the accurate preliminary work carried out in the laboratory prior to the in situ campaign can overcome these limitations. In fact, observations coming from a manifold of analytical techniques, each overcoming intrinsic limitations of the others, can provide extensive and complementary information. In addition, since non-invasive measurements do not require any contact with the examined object, they can be carried out all over the painted surface on a virtually infinite number of points, obtaining numerous integrative and representative data. Finally, the preparatory work carried out in the laboratory on mock-up samples allows a better understanding of the spectra to be achieved, and interpretation models to be built which include matrix effects. In conclusion, when all this information is jointly analyzed, a more thorough understanding of the paint chemical composition can be achieved than in the case of laboratory analyses on few samples, often consisting of specimens sampled from the borders of lacunae or close to the frame.

In this section, the analytical technique most frequently applied for non-invasive in situ investigations are introduced and, for each, advantages and limitations are presented. The techniques are: X-ray fluorescence (XRF), mid- and near Fourier transform infrared (FTIR) analysis in reflection mode, Raman spectroscopy (with and without a microscope), ultraviolet–visible–near infrared (UV–Vis–NIR) absorption and fluorescence spectroscopies, and X-ray diffraction (XRD).

## 2.1 X-ray Fluorescence

X-ray fluorescence (XRF) spectrometry allows for a rapid determination of the elemental composition of a material. The technique is particularly efficient for the study of high- $Z$  elements in low  $Z$ -matrixes. As a mobile tool, it has been extensively used for analysis in art and archaeology since the early 1970s and, therefore, represents the first technique to be historically exploited for intensive in situ non-invasive investigations [13–15].

Today, it is a primary tool universally exploited as a first approach to any study carried out in situ. Throughout the years, it has provided answers to a huge number of questions regarding manufactures in art, revealing specific aspects of the working practice of ancient masters [16–18].

A main limitation of XRF for in situ analyses is that only qualitative results are generally obtained, because matrix effects related to diffusion, re-absorption, and Auger ionization do not allow for reliable quantifications. This is particularly true in the case of complex layered structures, as occurs in paintings. Only in few favourable cases, has the modelling of the X-ray's absorption through different layers allowed for determining composition and thickness of paint layers on the basis of  $K\alpha/K\beta$  or  $L\alpha/L\beta$  intensity ratios. This method was successfully applied in situ to estimate the thickness of layers in a painting by Marco d'Oggiono, a pupil of Leonardo da Vinci, and on the *Mona Lisa* in the Louvre Museum, to determine how Leonardo achieved a barely perceptible gradation of facial tones from light to dark (the Leonardo *sfumato*) [19–21].

## 2.2 Reflection Infrared Spectroscopy

Reflection FTIR spectroscopy, from the near-IR (NIR) range up to  $400\text{ cm}^{-1}$ , is the most informative and reliable molecular technique among the MOLAB array of methods [22–32].

In the medium infrared range (mid-FTIR,  $4000\text{--}400\text{ cm}^{-1}$ ), the matrix effect appears with large spectral distortions, both in band shape and position, that can affect the interpretation of reflection spectra [33, 34]. Reflection mid-FTIR spectroscopy from a complex and optically thick surface (as that of a painting) generally includes the collection of both diffuse (from the volume) and specular (from the surface) reflection with a variable and unpredictable ratio that basically depends on the roughness of the examined surface as well as on the optical properties of the investigated materials. In particular, the specular reflection is governed by Fresnel's law and, accordingly, is a function of both the absorption index ( $k$ ) and refractive index ( $n$ ) [35]. As a consequence, reflection spectra of organic compounds typically show derivative profiles (resembling the refractive index dependence on wavenumber), while reflection spectra of many inorganic compounds (sulfates, carbonates, phosphates, silicates, etc.) are often distorted by the inversion of those fundamental bands that show  $k \gg n$  [28].

On the other hand, the diffuse reflection is governed by Kubelka–Munk's law and depends on the absorption index and scattering coefficient ( $s$ ). In diffuse reflection,

the spectral distortions are smaller and concern mainly the relative intensity of bands. Typically, weak absorption bands increase in their relative intensity with respect to stronger absorption bands especially when laying at high wavenumbers. Consequently, overtones and combination bands, usually neglected in transmission mode can be profitably exploited in reflection mode with substantial advantage, especially when the fundamental bands of the fingerprint regions are obscured by overlap with other signals [27, 28]. Moreover, diffuse reflection can also determine the enhancement of absorption bands related to minor components, allowing (in favourable cases) for a fine discrimination between pigments made of similar main chemical structure, as, for example, natural and synthetic ultramarine blue [36] or lamp and bone black [23].

In the NIR region (near-FTIR, 7000–4000  $\text{cm}^{-1}$ ), reflection spectra are dominated by diffuse (volume) reflection because the absorption indices of materials are generally rather low. As a drawback, near-FTIR spectra generally show poor specific profiles generated by an overlap of overtone and combination modes. Nevertheless, this spectral range proved to be useful for a non-invasive, initial classification of binding media and other natural polymers [37, 38].

Another important advantage is related to the higher penetration depth of near-FTIR with respect to mid-FTIR that makes it sensitive and exploitable to also characterize the binding media in the presence of a (preferably thin) layer of varnish, whose signal would prevail in the mid-infrared range.

A wide database of reflection spectra recorded on model paints composed of a variety of pigments and binders (different materials and different surface roughness) allowed distinctive information to be registered and classified, suitable for a correct interpretation of the mid- and near-FTIR spectral features during diagnostic campaigns [22–34].

Great advantage of portable FTIR instrumentation (mid and near) lies in the good performances of the available mobile instruments, that are comparable to those of standard bench-top equipment.

### 2.3 UV–Vis–NIR Absorption and Emission

UV–Vis–NIR reflection spectroscopy (typically in the range 190–1700 nm) in configuration with optical fibres (known as FORS—fiber optic reflectance spectroscopy) is a well-established technique for the characterization of pigments and colorants in works of art. It has the advantage of being easy to apply and it requires short acquisition times (few seconds). In addition, there is a wide commercial availability of truly portable and relatively inexpensive instrumentation.

Despite the advantages, some shortcomings prevent the reliable use of FORS as a self-consistent analytical tool. In particular, reflectance spectra in the UV–Vis–NIR range features broad bands related to electronic transitions (besides a few vibrational bands in the NIR) and, therefore, they have an intrinsically lower fingerprinting ability when compared with spectra obtained with other molecular spectroscopic techniques, such as FTIR or Raman spectroscopy. However, although in some cases it cannot allow unambiguous identification, its straightforward

applicability makes it an ideal spectroscopic method in a multi-technique analytical approach.

Early publications on the topic (without optical fibres) date back to the 1930s [39]. Since then, it has been widely used alone (typically applied with extension to the NIR range up to 2500 nm) or in combination with other techniques for the study of paintings [40–42] and illuminations in manuscripts [43–45].

More recently, UV–Vis–NIR fluorescence spectroscopy has been exploited as an additional non-invasive tool to investigate coloured materials in paintings, manuscripts and other polychromies [46]. Its use is particularly advisable when organic dyes and/or pigments are present with rather good emission quantum yield. As for absorption electronic bands, the corresponding emissions are usually quite broad (i.e. several tens of nanometers full width at half-maximum, [FWHM]). This often causes overlapping among emissions from distinct fluorophores and makes it difficult to distinguish among them, thus reducing the specificity of spectrally based discrimination. In addition, the spectral properties of a fluorophore can vary depending on its microenvironment (e.g. binding media, mixture with other pigments) with further complications. Nevertheless, on the basis of in-depth studies in the laboratory (in solution, solid state and, finally, on paint models) it has been demonstrated that its fluorescence properties may be used to identify anthraquinone dyes (differentiating between those of animal or vegetal origin) [47], oxazines [48], indigoids [49], flavonoids and carotenoid dyes [50]. In addition, a few inorganic pigments (e.g. zinc white [51], Cd-based pigments [52, 53], and Egyptian blue [54]) show rather specific emission bands (the latter two in the NIR range) which can be exploited for their non-invasive identification.

Here, the limitations produced by matrix effects are related to self-absorption, that is, absorption by the fluorophore itself of the emitted light, thus erasing a variable portion of the emission spectrum on the short wavelength side. The problem of the correction for self-absorption of fluorescence spectra collected on pictorial works has been addressed, and a method for the treatment of the fluorescence signals has been first developed for luminophore dispersed in an opaque layer [55] and then extended for luminophore in a translucent layer on a coloured background (i.e. glazing technique) [56].

With the aim of increasing the specificity of emission UV–Vis–NIR spectroscopy toward the molecular recognition of dyes and organic pigments, the exploitation of fluorescence kinetic parameters has been recently proposed. In fact, kinetic analysis of emission decay curves can be used to distinguish among different compounds that have similar fluorescence spectra and may aid in the identification of the molecular species by comparison with known standards [57, 58].

Notably, a prototype system for integrated measurements of UV–Vis–NIR reflection spectroscopy (investigating the absorption properties), steady-state fluorescence, and luminescence lifetimes is currently applied in MOLAB interventions to record on the same spot, *in situ*, the full photo-physical behaviour of dyes and pigments on painted surfaces [59].

## 2.4 Raman Spectroscopy

Drawbacks and successes of portable Raman spectrometers for in situ non-invasive applications have been widely discussed in a recent review paper with a rich, extended bibliography [60]. Much more than for bench-top applications, molecular fluorescence represents the main inconvenience for non-invasive Raman spectroscopy, especially when analysing paint layers rich of (oxidised) organic components. In the case of a micro-spectrometry setup, no portable confocal microscopes are available and this implies the occurrence of matrix effects producing a high fluorescence background that obscures the weak Raman features. This limitation is obviously also present in the case of direct use of optical fibres (i.e. measurements without a microscope).

Other inconveniences arise from the compactness of portable systems, implying a reduced optical path and, therefore, a lower spectral range and resolution than in bench-top instruments. Furthermore, shields or correction systems for the daylight are not always available and, in case of use of scaffoldings, vibrations of the support of the spectrometer can seriously impede the recording of spectra. A final relevant drawback is that extreme attention must be paid in regulating the laser power, since the surface of the artefacts may be thermally and/or photochemically altered. This is obviously valid both for portable and bench-top instrumentation; however, it is evident that measurements carried out directly on the surface of a precious artwork (i.e. a painting masterpiece) require much more caution than laboratory investigation on samples. This calls for careful preliminary studies prior to the in situ campaign to search for the best compromise between safety of operation and intensity of scattering signals [61].

In general, Raman spectroscopy has proved to be a very successful technique for in situ studies of illuminations in manuscripts (low fluorescence, due to the generally high pigment/binder ratio), glasses, enamels, metals, but less for panel and canvas paintings. In case of mural paintings, the diffuse presence of organic protectives and/or consolidants, applied in restoration, as well as problems related to vibrations and defocusing, still usually limits in situ Raman spectroscopy applications.

As for bench-top instruments, to overcome fluorescence, a great advantage is offered by the use of high-wavelength lasers, which are able to reduce or eliminate electronic excitation, as, for example, those at 785 nm (diode laser) or those more recently introduced in a portable dispersive setup emitting at 1064 nm (Nd:YAG laser). However, due to the  $\nu^4$  dependence of Raman intensity, the sensitivity of spectra acquired using a near-infrared excitation is generally very low.

## 2.5 X-ray Diffraction

XRD is the most reliable method for the identification of minerals or synthetic crystalline materials. In principle, it represents the fundamental technique to complement chemical analyses by XRF and vibrational spectroscopy (FTIR and Raman). However, applications of portable XRD systems for in situ non-invasive measurements are scarce, mostly due to the severe geometrical restrictions of the in situ experimental setups that introduce numerous drawbacks. The characteristics

of existing XRD systems for heritage applications have been recently reviewed and the performances of each system compared [62]. These instruments are, apart from two single cases, based on angular dispersion XRD (AD-XRD) and consist of conventional goniometer-type diffractometers in which data are obtained by scanning the detector and/or the X-ray source [62–64], or systems that make use of two-dimensional (2D) detectors, such as charge-coupled devices (CCDs) [65, 66] or imaging plates, [67–69] that allow for the recording of diffraction data without mechanical movements.

The positioning of the instrument with respect to the surface to be analyzed is a critical parameter. For example, referring to the two latter systems, the source (a selectable X-ray tube) illuminates a small spot on the sample surface at  $10^\circ$  incidence and the 2D detector is set at the nearest distance from the spot. Thus, steric hindrances inevitably introduce limits in the  $2\theta$  angular range of the detected signals, which are  $10^\circ$ – $60^\circ$  and  $20^\circ$ – $55^\circ$  for the two systems, respectively, with  $0.25^\circ$ – $0.3^\circ$  angular resolution [41]. A higher  $2\theta$  scan range ( $24^\circ$ – $134^\circ$ ) with  $2\theta$  resolution of  $0.12^\circ$  is available in another system that uses a goniometer. However, the beam size that defines the spatial resolution is higher [62]. In all cases, due to the low intensities of the diffracted beams, in situ XRD analyses require acquisition times that are much longer than for the other non-invasive techniques, amounting to 30 min or even much more, sometimes hours, to achieve one single acceptable spectrum. A final drawback of non-invasive XRD is that shifts of the diffraction  $2\theta$  angles can be recorded, mainly due to the different depth of the crystals of the minerals to be detected (e.g. the crystals of the pigments). This is a disadvantage that, in principle, could be turned into an advantage when information on the depth of the pigment layers is required [70].

The advantage of XRD is that the technique is well established, diffraction phenomena are theoretically well understood (data can be theoretically simulated from crystal structure data), and a complete reference database is available as a powder diffraction file (PDF) supplied by the International Centre for Diffraction Data (ICDD). All these features make XRD a profitable technique to complement the data acquired in situ by FTIR and Raman spectroscopy, provided that a long-term analytical campaign is planned (several days), due to the requested long accumulation time for each point of measurement.

A drastic reduction of the data acquisition time (one or two orders of magnitude) is, in principle, possible when energy dispersive XRD (ED-XRD) is used, based on polychromatic excitation (using the *brehmstrahlung* X-rays that are filtered off in conventional X-ray tubes) and X-ray energy dispersive detection (i.e. using the same detector for XRF measurements). This approach represents a possible alternative to AD-XRD for in situ heritage applications [70–73]. However, in this approach, some complications arise: first, the quantities that regulate the scattered intensity depends on the energy; second, the spectral resolution depends not only on the angular divergence of the X-ray beam, but also on the energy resolution of the detector; third and most important, XRD and XRF peaks are recorded together in the same spectrum, sometimes overlapping, an inconvenience that can be avoided by changing the detection angle, reintroducing in some way the necessity of a mechanical angular movement. For these reasons, instruments able to carry out both



angular and energy dispersive XRD have been assembled with the purpose of taking advantages of both ED-XRD (shorter time and higher energy penetration) and AD-XRD (higher d resolution).

The first in situ application of a double ED and AD-XRD system was carried out in Japan to investigate a bronze mirror from the Eastern Han Dynasty (25–220 AD) and the painted statue of “Tamonten holding a stupa” from the Heian Period (794–1192 AD) [71]. Two new prototypes have been very recently set up and successfully tested at ICP-Elettra, showing promising results [73].

### 3 In Situ Experimental Results

MOLAB has been operative in Italy and Europe for around 15 years (started in 2001, with a national project dedicated to the monitoring of the state of conservation of the David of Michelangelo [74]) and, during these years, great experience has been accumulated with a total number of more than two hundred studies on different types of heritage artworks, including paintings, bronze and stone sculptures, manuscripts, and ceramics [12].

On the basis of this experience, selected examples of results are presented in this section on the identification of pigments, dyes, and binders in paintings. It will be also shown how an important, key passage for the success of the MOLAB measurements is represented by the preliminary work developed in the laboratory prior to the in situ campaign.

Using a protocol that starts with XRF measurements, followed in the order by (a) near- and mid-FTIR, (b) UV–Vis absorption and emission, (c) Raman spectroscopy, and (d) XRD, it can be assessed that the general characterization of the execution technique of a painter [identification of pigments and family of binder(s)] can be achieved today through direct measurements on the work of art, without any sampling. The necessity of a few micro-samples is restricted to the solution of specific problems, as the characterization of the paint stratigraphy or the determination of the detailed nature of binder(s) and colorants [22–25].

Successful applications of in situ non-invasive approaches for the study of painting techniques have been carried out on masterpieces of different periods and schools, as Renaissance paintings by Raphael [16], Perugino [17], Leonardo, on impressionist and post-impressionist paintings by Cézanne [25], Renoir [23] and Van Gogh [3, 75, 76], and on contemporary paintings by Picasso [77], Burri [78] Mondrian [79], De Stael, and many others.

#### 3.1 Non-invasive Characterization of Pigments

##### 3.1.1 Identification of Ancient Masters' Palette

Among these studies, an exemplary characterization of ground and pigments has been carried out at the Royal Museum of Fine Arts of Antwerp on the triptych *Christ among Singing and Music Playing Angels* by the Flemish painter Memling [80]. The painting, dated ca. 1487–'90, is composed of three panels (ca.



**Fig. 1** The mobile laboratory, MOLAB, during the campaign at the Royal Fine Art Museum of Antwerp for the study of the triptych *Christ among Singing and Music Playing Angels* (ca. 1487–90), by H. Memling. The analytical work is proceeding simultaneously applying different techniques. The instruments rotate in front of each panel in order to investigate the selected areas with all the available equipment

2 m × 1.5 m, each) which depict Christ in the clouds, surrounded by 16 angels, singing and playing different musical instruments. The study has been carried out through a long-term analytical campaign, in occasion of the restoration of the painting, when the varnish was removed. In Fig. 1, the MOLAB laboratory setup at the Royal Museum of Fine Arts is shown.

Together with XRF, reflection mid- and near-FTIR, absorption and emission (steady-state and time-resolved) UV–Vis spectroscopies, and XRD were exploited. Non-invasive Raman spectroscopy was not used in this case, because scattering was fully covered by a large fluorescence background induced by the binding medium.

Preliminary to the study of pigments, the presence of a small lacuna (ca. 0.2 cm<sup>2</sup>) in the paint, that left the underlying ground uncovered (Fig. 2), permitted the materials in the ground layer(s) to be first investigated by mid-FTIR and XRD, without interferences from the paint. The presence of both gypsum (CaSO<sub>4</sub>·2H<sub>2</sub>O) and chalk (CaCO<sub>3</sub>) in the ground layers was clearly revealed by mid-FTIR through the combination and overtone bands at 2200 [27] and 2500 cm<sup>-1</sup>, [25, 81] respectively. XRD spectra, collected in these areas, confirmed the presence of both compounds, as shown in Fig. 2.

The discovery of gypsum was rather unexpected. According to this finding, Memling here combined the practice of the Western and Northern European artists to use chalk for the ground, with the habits of the Mediterranean School, known to employ gypsum for the same purpose [82]. Although it remains not fully established if the two compounds were mixed or separated in two layers, the occurrence of gypsum as a preparation layer was confirmed by FTIR measurements which clearly indicated the presence of calcium sulfate not only from areas with emerging ground (lacunae), but also from several undamaged areas, through the paint (see, for

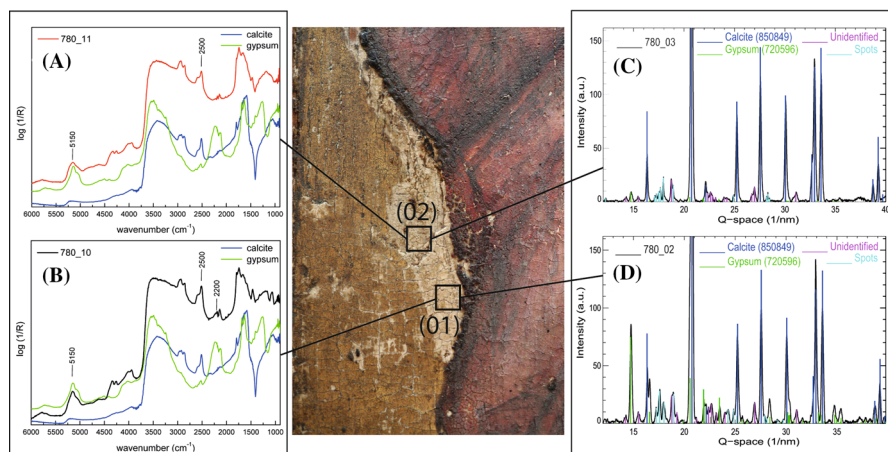


**Fig. 2** Identification of calcium carbonate and gypsum by both mid-FTIR (a, b) and XRD (c, d) from two areas (01 and 02) of a lacuna in the paint in Fig. 1 (modified from Ref. [80])

example, the spectra reported in Fig. 3: a broad signal at  $5150\text{ cm}^{-1}$ , ascribable to OH combination band of hydrated calcium sulphate [27]).

The figures represented in the three panels of the painting were characterised by a wide variety of colours and shades that were achieved by the painter combining different pigments. The variegate chromatic effects were created through specific mixtures or overlayers, especially on the wings and robes of the playing and singing angels.

Essential for the unambiguous molecular identification of pigments and mixtures in these complex areas was the complementary information originated from mobile FTIR, XRD, and UV–Vis absorption and emission spectroscopy. It was found that in the wings and robes of the angels, shades from light blue to deep purple were achieved by combining azurite,  $2\text{CuCO}_3\cdot\text{Cu}(\text{OH})_2$  (identified by FTIR and XRD) with a variety of other pigments, such as bone black (identified by FTIR), lead white (revealed by FTIR and XRD), lead–tin yellow type I (revealed by XRD) and/or an organic red lake, most probably madder lake (identified by UV–Vis absorption and emission spectral profiles).

These pigments, together with natural ultramarine (present only in precious details), cinnabar and/or red ochre (in the incarnates), yellow, and brown ochre composed the full palette of the painter.

In more detail, azurite was characterized by reflection mid-FTIR via the combination bands of both the copper carbonate (structured signal at  $2500\text{ cm}^{-1}$ ) and copper hydroxide moiety (doublet at  $4244$  and  $4373\text{ cm}^{-1}$ ) [28] (see Fig. 3); lead white was mainly identified by the  $\nu_1 + \nu_3$  combination band of cerussite ( $\text{PbCO}_3$ ) and hydrocerussite [ $2\text{PbCO}_3\cdot\text{Pb}(\text{OH})_2$ ] at  $2410$  and  $2428\text{ cm}^{-1}$ , respectively; while carbon black of animal origin was identified through a small sharp signal at  $2010\text{ cm}^{-1}$  [28].

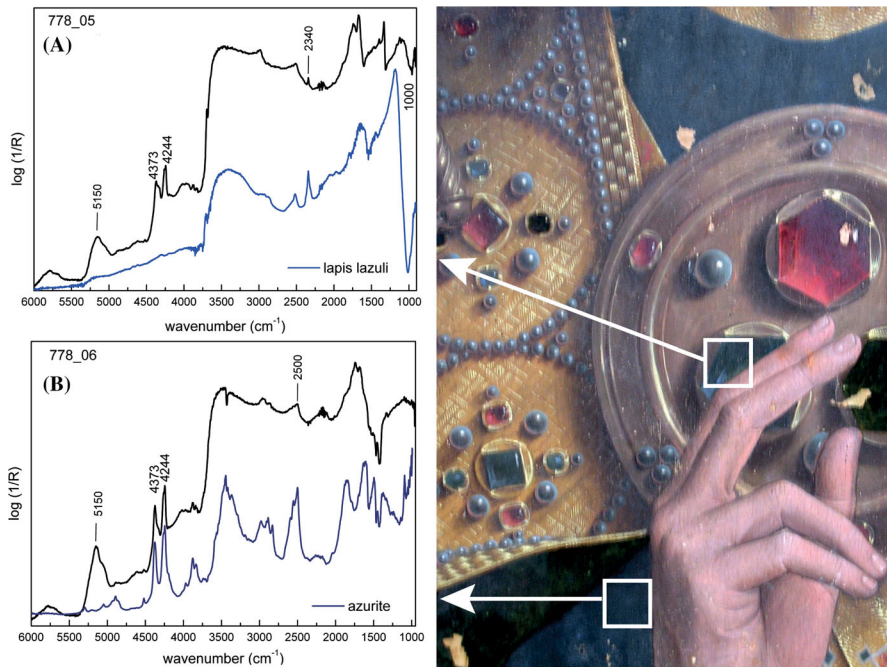


**Fig. 3** Mid-FTIR reflection spectra recorded on two areas of the garment of Christ (see Fig. 1). Spectrum A (black line) illustrates the presence of both azurite and natural lapis lazuli in the highlights of the blue gems, while only azurite was found to characterise the blue colour of the garment (spectrum B, black line). Blue lines reference spectra of lapis lazuli and azurite (modified from Ref. [80])

XRD ascertained and confirmed the presence of the mineral azurite in the wings and robes of most of the angels and the presence of both hydrocerussite and cerussite in lead white. In dark blue areas of the robes, where mid-FTIR spectra showed the presence of carbon black, XRD established the presence of graphite, intermixed with the blue paint to produce a darker shade.

The combined use of XRF and XRD also indicated that the feathers in the rainbow-coloured wings of some angels were obtained by combining azurite with lead–tin yellow. The latter pigment, not visible by reflection FTIR spectroscopy, was also found in lighter yellow areas, on the mantle of one of the angels, where a combination of Pb and Sn was revealed by XRF, and XRD ascertained the presence of a crystalline phase of lead–tin oxide, in particular, lead–tin yellow type 1.

Examinations of deep purple areas suggested that this colour was obtained by combining azurite with a red organic pigment (layered and/or intermixed). Reflection UV–Vis emission and absorption spectroscopy succeeded in specifying the vegetal origin of an anthraquinone dyestuff, representative of madder lake. This lake was identified by the structured shape of the absorption band, with typical features at 510 and 540 nm, as well as the maximum of the emission band at 600 nm (Fig. 4) [47, 59]. The identification was also confirmed by the time decay

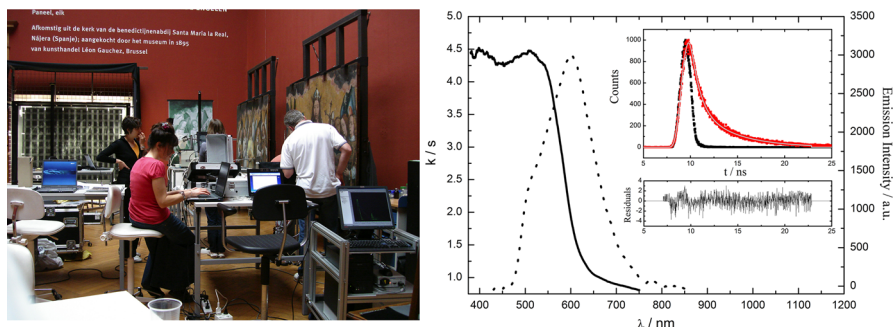


**Fig. 4** *Left* preparation of the measurement with the portable system for absorption/fluorescence measurements. *Right* absorption (full line) and fluorescence emission spectra (dotted line) recorded in a deep purple area. In the inset, fluorescence decay time (red dots), excitation source (black dots), fitting curve (thin grey line), and distribution of residuals (bottom). Excitation wavelength:  $\lambda = 455$  nm. Emission max.  $\lambda = 620$  nm (rearrangement from Ref. [80])

values that were of ca. 1 and 4 ns (1, 2 and 4.3 ns of standard madder lake in oil [57]).

Colours tending to orange, such as the feathers in the wing of one angel, were obtained by a combination of vermilion with lead–tin yellow, as demonstrated by XRD and XRF.

Light blue paint was obtained by combining azurite with variable ratios of lead white. However, mid-FTIR spectra collected on the highlights of the blue gems decorating the cloak of Christ, revealed together with azurite, a broader absorption band inverted by a *reststrahlen* effect, in the range  $900$ – $1100$   $\text{cm}^{-1}$ , corresponding to the Si–O antisymmetric stretching vibration, and a sharp stretching band at  $2340$   $\text{cm}^{-1}$  assigned to the  $\text{CO}_2$  stretching mode (Fig. 3). The distinctive incidence of silicates, together with the presence of  $\text{CO}_2$ , is an evident marker of the presence of natural lapis lazuli. The entrapment of  $\text{CO}_2$  in the  $\beta$ -cage of the sodalite framework of lazurite is related to the geological genesis of the mineral [36]. The presence of lazurite over-imposed to azurite was fully confirmed by the XRD spectra, recorded in the same area (data not shown).

A summary of the obtained results is reported in Table 1, with an indication of the analytical techniques relevant for the identification. In the table, the results obtained by MOLAB in the study of another triptych by H. Memling, *The Last Judgement* of the National Museum of Gdansk [83] are also reported. The comparison highlights a substantial analogy of the materials used by Memling in the two artworks.

In conclusion, it has been shown that the integration of elemental, vibrational, electronic, and XRD analytical techniques now permits a general description of the materials used by the artist to be obtained in situ without any sampling, with a satisfying identification of the inorganic pigments used, accompanied by good indications of the presence of organic pigments and colorants.

**Table 1** Hans Memling's use of pigments and ground from the MOLAB non-invasive studies of *Christ among Singing and Music Playing Angels* in the Royal Fine Art Museum of Antwerp and *The Last Judgement* triptych in the National Museum of Gdansk (Adapted from Ref. [83])

Area of interest	<i>Christ among Singing and Music Playing Angels</i> (Antwerp) [80]	<i>The Last Judgement</i> triptych (Gdansk) [83]	Analytical techniques <sup>1</sup>
Ground	Calcium carbonate and gypsum	Calcium carbonate	XRF, mid- and near-FTIR, XRD
Blue	Lapis lazuli (only gems of the Christ mantle)	Lapis lazuli (precious details)	Mid-FTIR, XRD
	Azurite (with black carbon in darker areas)	Azurite	XRF, mid-FTIR, XRD
	Smalt	–	XRF, near-FTIR
Green	Cu-based pigments	Cu-based pigments	XRF
	Azurite and lead–tin yellow	–	XRF, mid-FTIR, XRD
Yellow	Lead–tin yellow (I)	Lead–tin yellow (I)	XRF, XRD
	Yellow ochre	Yellow ochre	XRF, XRD, mid-FTIR
Red/orange	Cinnabar	Cinnabar	XRF, UV–Vis absorption
Purple	Madder lake	Madder lake	UV–Vis fluorescence emission (steady state and time resolved)
Brown	Ochre	Ochre	XRF, XRD
White	Lead white (hydrocerussite and cerussite)	Lead white (hydrocerussite and cerussite)	Mid-FTIR, XRD
Black	Bone black	–	Mid-FTIR
Incarnates	Ochre and/or cinnabar with lead white	Ochre and/or cinnabar with lead white	XRF, UV–Vis absorption, mid-FTIR, XRD
Gilding	Pure gold by mixtion or by bole, goethite and quartz	Pure gold by mixtion	XRF, XRD
Binder <sup>2</sup>	Lipidic (weak signal of proteins only in some areas with thin paint)	Lipidic (weak signal of proteins in some areas)	Mid-FTIR

<sup>1</sup> Portable XRD results refer only to the Antwerp painting<sup>2</sup> See Sect. 3.2 for details on binding media identification

### 3.1.2 Non-invasive Discrimination of Pigments Showing Varieties in Composition and Structures

The non-invasive in situ approach has been recently demonstrated to be suitable for the diagnostic identification of pigments that show varieties of compositions and structures. This is the case, for example, of the so-called lead antimonates, which are known to be characterized by a pyrochlore structure,  $\text{Pb}_2\text{Sb}_2\text{O}_7$  (Naples yellow), where the replacement of Sb by various elements gives rise to formulation varieties  $\text{Pb}_2\text{Sb}_{2-x}\text{Y}_x\text{O}_{7-x/2}$  ( $\text{Y} = \text{Sn}, \text{Zn}, \text{Fe}, \text{Pb}$ ) that correspond to different yellow hues [84–86]. This is also the case of the cadmium sulfide pigments, which share a common structure based on CdS, but partial substitutions of Cd or S with elements

as Zn, Hg, and Se lead to a variety of tonalities from yellow to orange and red [52, 53].

The discrimination among formulations and structures of these series of pigments, within the same family, is not straightforward, because their spectroscopic properties usually show strong similarities. In addition, XRD could not always be applied because synthetic historical pigments have often been prepared by imperfectly controlled reactions, producing not only crystalline but also highly disordered phases. In this case, the exploitation of vibrational spectroscopy can be particularly helpful, confirming FTIR and Raman spectroscopy in particular, as specifically suitable techniques for non-invasive in situ discrimination of the possible varieties.

The Raman spectrum of pure Naples yellow ( $\text{Pb}_2\text{Sb}_2\text{O}_7$ ) displays a typical feature, that consists of strong band at about  $510\text{ cm}^{-1}$  related to the symmetric stretching of the  $\text{SbO}_6$  octahedra [85]. The same Raman scattering mode, in a modified pyrochlore showing orange color, appears split in two bands, one again at  $510\text{ cm}^{-1}$  (but much less intense) and another around  $450\text{ cm}^{-1}$ , with further modifications occurring in the low wavenumber region. On the basis of a structural study on standards of lead antimonate yellows, these spectral features have been demonstrated to be distinctive of a doped pyrochlore with Sb partially substituted by Zn or Sn [86, 87].

Yellow CdS is a semiconductor with a direct band gap of 2.41 eV (512 nm at room temperature) [88] whose color can be tuned from yellow to light-yellow hues by partially substituting cadmium with zinc in the crystal lattice, thus forming solid solutions of cadmium zinc sulfide ( $\text{Cd}_{1-x}\text{Zn}_x\text{S}$ ) [89]. Alternatively, co-precipitation with variable amounts of selenium leads to the formation of cadmium sulfo-selenide solid solutions ( $\text{CdS}_{1-x}\text{Se}_x$ ) characterized by tonalities ranging from orange to red [89]. The resonance-enhanced longitudinal optical Raman modes have been shown to be linearly dependent on the Se and Zn molar fraction of the ternary solid solutions. These linear relationships are exploitable for the in situ identification of the composition of ternary pigments by resonance Raman spectroscopy.

In addition to these cases, the study of lead chromates and lead chromate–sulfate co-precipitates has attracted specific interest, since their possible identification via vibrational spectroscopy (i.e. IR and Raman) and XRD. These substances compose the series of pigments known as chrome yellows that were often used by painters of the late nineteenth century, as the impressionists and post-impressionists. They show tonalities that range from yellow-orange to pale-yellow according to their chemical composition ( $\text{PbCrO}_4$ ;  $\text{PbCr}_{1-x}\text{S}_x\text{O}_4$ , with  $0 < x < 0.8$ ) [90, 91]. Another form of lead chromate-based pigment is the co-precipitate with lead oxide and is commonly known as chrome orange [ $(1-x)\text{PbCrO}_4 \cdot x\text{PbO}$ ] due to its deep orange shade.

From the crystallographic point of view,  $\text{PbCrO}_4$  and chrome orange show monoclinic structures, while that of  $\text{PbSO}_4$  is orthorhombic. It follows that a structural change in  $\text{PbCr}_{1-x}\text{S}_x\text{O}_4$  co-precipitates is observed with increasing sulfur content: when  $x$  exceeds 0.4–0.5, a modification from a monoclinic to an orthorhombic structure takes place [95, 96].

Van Gogh himself, in the letters to his brother Theo and to his friend Emile Bernard (letters n. 593, 595, 684, 687, 710, 863), mentions the use of three varieties of lead chromate-based pigments, namely chrome yellow types I, II, and III, probably corresponding to pale-yellow (S-richer  $\text{PbCr}_{1-x}\text{S}_x\text{O}_4$ ), yellow-orange ( $\text{PbCrO}_4$ ) and orange  $[(1-x)\text{PbCrO}_4 \cdot x\text{PbO}]$  hues [92–94].

It has been demonstrated that the darkening observed for chrome yellows, caused by the photo-reduction of original chromates to Cr(III) compounds, is favoured when the pigment is present in the orthorhombic S-rich form  $\text{PbCr}_{1-x}\text{S}_x\text{O}_4$  ( $x > 0.4$ ) [75, 95–98]. Thus, the possibility to distinguish among different forms of lead chromate-based pigments and to map their location all over the surface of a painting is relevant for the assessment of the areas subject to a major risk of degradation.

In  $\text{PbCr}_{1-x}\text{S}_x\text{O}_4$  solid solutions, the chromate to sulfate substitution leads to a volume decrease of the monoclinic unit cell at a low sulfate concentration and to a change of the crystalline structure from monoclinic to orthorhombic with increasing sulfur content. These modifications strongly affect the fundamental vibrational bands of these materials (with changes of shape and wavenumber position of these signals), making Raman and infrared spectroscopies suitable techniques for their direct discrimination, even when using a non-invasive in situ approach.

As is visible in Fig. 5, in the Raman spectra collected by a portable instrument with a 785 nm laser excitation on a series of paint models, the chromate bending multiplet [ $\nu_2/\nu_4$  ( $\text{Cr}_2\text{O}_4^{2-}$ )] appears to be strongly affected by the sulfate substitution, showing a clear shift of band positions and a modification of band shapes related to the change of the crystalline structure. Additionally, the symmetric stretching band of both sulfate [ $\nu_1(\text{SO}_4^{2-})$ ] and chromate [ $\nu_1(\text{CrO}_4^{2-})$ ] moieties shifts slightly toward higher energy, as a function of the sulfate amount. Another relevant effect of the chromate to sulfate substitution is the decrease of the Raman scattering cross-section.

Based on the knowledge developed by the study of the laboratory model paints, non-invasive Raman spectroscopy has been successfully applied in situ to study a series of paintings by Van Gogh conserved at the Van Gogh Museum in Amsterdam, namely *Sunflowers gone to seed*, *Bank of the Seine*, and *Portrait of Gauguin* (Fig. 5). In *Sunflowers gone to seed*, the spectrum acquired from a yellow-orange area shows the presence of monoclinic  $\text{PbCrO}_4$ . The spectrum from a greenish yellow area of *Bank of the Seine* shows again the spectral features of the monoclinic  $\text{PbCrO}_4$ , with the additional presence of a signal at  $1050\text{ cm}^{-1}$  indicating a mixture with lead white. Finally, in a light yellow area of *Portrait of Gauguin*, the chrome yellow pigment is identified as the unstable S-rich  $\text{PbCr}_{1-x}\text{S}_x\text{O}_4$  ( $x \sim 0.5$ ). The presence of the sulfate component is well-evidenced by the  $\nu_1(\text{SO}_4^{2-})$  band at  $976\text{ cm}^{-1}$  and changes of shape and positions of  $\nu_1(\text{CrO}_4^{2-})$  and  $\nu_2/\nu_4$  ( $\text{Cr}_2\text{O}_4^{2-}$ ) modes.

The presence of lead chromates and unstable lead chromate–sulfate co-precipitates has been recently found by non-invasive in situ measurements also on the Van Gogh's famous *Sunflowers* painting, in the Van Gogh Museum of Amsterdam [76].

These results unequivocally demonstrated that Van Gogh employed different types of lead chromate–sulfate solid solutions, either in undiluted form or in



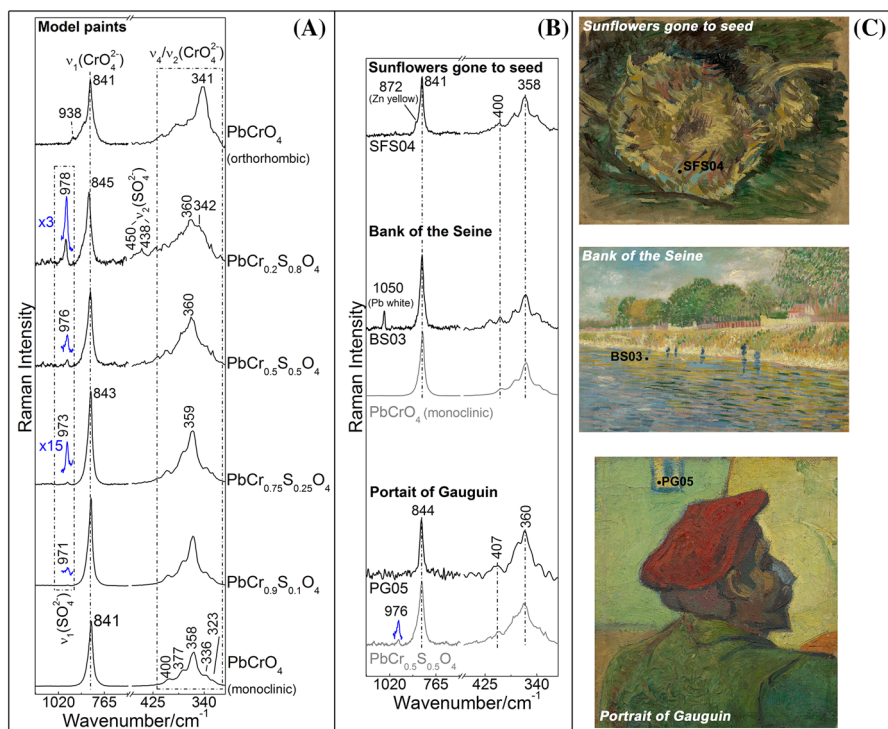


**Fig. 5** Raman spectra collected using the MOLAB portable device (excitation line  $\lambda = 785.0$  nm) from: **a** oil paint model samples made up of different chrome yellow pigments with different compositions and structures and **b** from yellow areas of the paintings *Sunflowers gone to seed*, *Bank of the Seine* and *Portrait of Gauguin* by Vincent van Gogh (all at the Van Gogh Museum in Amsterdam). **c** Photo of the paintings (from top to bottom) with indication of the corresponding in situ Raman spectroscopy measurement points (rearrangement from Ref. [61])

mixtures with other pigments (such as lead white, as shown above, red lead and vermilion). He also used other chromate-based compounds such as chrome orange  $[(1-x)\text{PbCrO}_4 \cdot x\text{PbO}]$  and zinc yellow  $(\text{K}_2\text{O} \cdot 4\text{ZnCrO}_4 \cdot 3\text{H}_2\text{O})$ . All such information are essential to curators to implement adequate measures of preventive conservation [99].

### 3.1.3 Identification of Synthetic Organic Pigments

The synthetic manufacture of organic dyes was greatly developed following the discovery of Perkin's mauve in 1856, distinguishing routes to produce brightly colored lake pigments which were widespread from the late nineteenth century. These lakes were later supplemented by the introduction of the first water-insoluble organic pigments, namely the  $\beta$ -naphthol pigments, and then many others [100]. It is due to their wide use in contemporary paintings that the identification of synthetic dyes attracted considerable interest in recent years, leading to a source of literature exploiting the use of various chromatographic and spectro analytical techniques,

namely high-performance liquid chromatography (HPLC), infrared and Raman spectroscopy techniques [79, 101–104].

Mobile Raman spectroscopy can give a decisive contribution to the identification of synthetic organic pigments when used in integrated applications with other mobile techniques as XRF and FTIR. For example, identification of red azo  $\beta$ -naphthols occurred in an extensive campaign by MOLAB on paintings by Alberto Burri dating from 1948 to 1975, belonging to the Collezione Albizzini (Cittá di Castello, Italy). Within the campaign, the use of synthetic red organic pigments by Burri was identified in two paintings, *Rosso* (1950) and *Rosso Gobbo* (1954), exploiting data from in situ XRF, FTIR and Raman spectroscopy (using a portable micro-setup equipped with a 532 nm laser excitation).

In the painting *Rosso* (1950), the generic presence of a red organic pigment was revealed by UV–Vis fluorescence, which showed a maximum emission around 630 nm. Being, however, insufficient to identify the nature of the pigment, the study was deepened by exploiting a combination of non-invasive XRF and mid-FTIR techniques. By XRF examination, these areas showed a weak but clear amount of chlorine, whose presence was strictly related to the observed red regions (Fig. 6a, gray line). The same areas, examined by mid-FTIR in reflection mode, revealed specific distorted bands, consisting of derivative-like bands that corresponded to those observed on both reflection and transmission spectra on the standard of pigment red 4 (PR4; Fig. 6b).

This pigment is one of the four commercially available red azo  $\beta$ -naphthols, PR1, PR3, PR4, and PR6, which are characterized by a common structure where the azo function ( $-N=N-$ ) is bound to a naphthol group and to a 2,4-substituted aromatic ring which features different substitutions for each pigment [100]. In particular, only PR4 (chlorinated para red) and PR6 (parachlor red) show chlorine as an aromatic ring substituent, although in different positions. This finding allowed the presence of PR1 and PR3 to be excluded in the examined painting, circumscribing the possibilities to PR4 or PR6. In spite of the fact that the FTIR spectrum recorded on *Rosso* showed features very similar to those of the PR4 standard and in agreement with literature data [103], the lack of a reference infrared spectrum of the positional isomer PR6 did not allow a discrimination of the two pigments with absolute certainty.

In another painting of Burri, *Rosso Gobbo* (1954), mid-FTIR spectroscopy suggested the possible presence of the same red organic pigment. However, more diverse than in the previous case, no secure PR4 distinctive features appeared in FTIR (see Fig. 6b, black line) nor in XRF spectra, where a peak at 2.65 keV corresponding to the chlorine  $K\alpha$  emission (Fig. 6a, inset) was too weak to be assigned to chlorine with certainty. While XRF and FTIR did not permit an unambiguous identification, here, micro-Raman spectroscopy measurements on the same areas of the painting (Fig. 6c, black line) showed scattering features very similar to those of the two red azo  $\beta$ -naphthols PR4 and PR3 (Fig. 6c, gray and light gray lines). Further comparison of the recorded spectra with the standards indicated that the observed strong signal at about  $1580\text{ cm}^{-1}$  is present in PR4 and absent in PR3. Furthermore, following Raman spectroscopy literature data [103, 104] it has been possible to distinguish between the red azo  $\beta$ -naphthol pigments PR4 and PR3

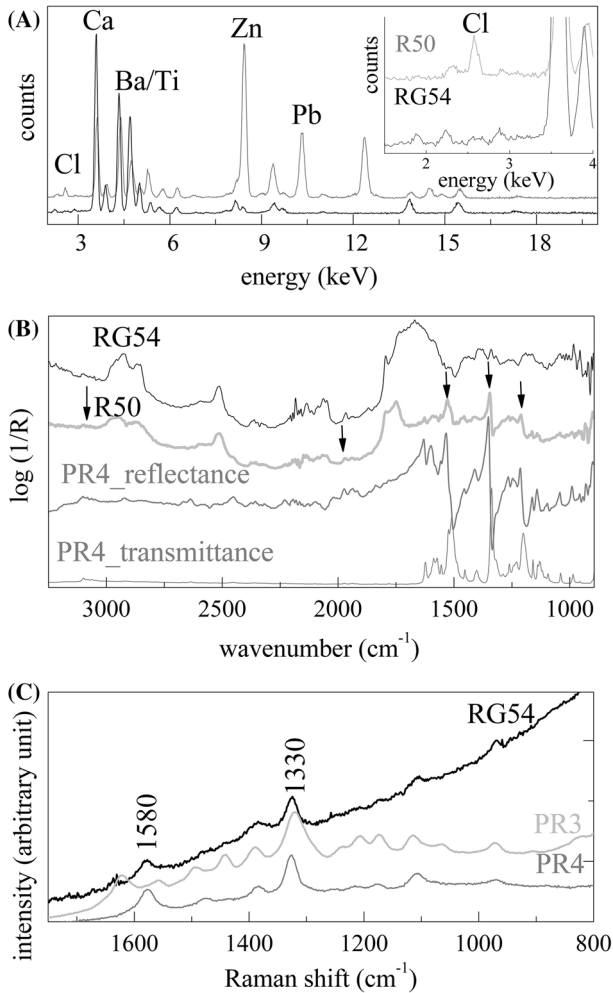


**Fig. 6** XRF spectra recorded on red areas of the paintings *Rosso* (R50 gray line) and *Rosso Gobbo* (RG54 black line) by A. Burri; *inset* enlarged view of the energy range 1.5–4 keV; **b** reflection mid-FTIR spectra collected on the red areas of the paintings *Rosso* (R50 gray line) and *Rosso Gobbo* (RG54 black line) compared with the reflection and transmission mid-FTIR spectra of PR4 standard; **c** micro-Raman spectrum collected on a red area of the painting *Rosso Gobbo* (RG54 black line) compared with the spectra of PR3 (light gray line) and PR4 (gray line) standards (from Ref. [78])

based upon the relative intensities of the intense bands at about 1330 and 1200  $\text{cm}^{-1}$ . These findings lead to the exclusion of *toluidine red* (PR3) and also *para red extra light* (PR1), which are characterized by different ring substitutes and different Raman spectroscopy scatterings, confirming the use by Burri of the *chlorinated para red* (PR4) or the positional isomer *parachlor red* (PR6).

It should be mentioned that the identification of highly fluorescent natural and synthetic organic dye components, often encountered in ancient, modern, and contemporary paintings respectively, provide a challenging analytical task for

conventional Raman spectroscopy in a non-invasive set-up as well as bench-top applications. For this reason, in recent years, the potential of surface-enhanced Raman spectroscopy (SERS) methodologies for the ultrasensitive detection of organic dyes, colorants and pigments used by artists has been widely exploited and appreciated. The introduction of this analytical tool in the field of heritage research has significantly improved the chances of successfully identifying dyes on minute samples. Furthermore, research efforts have been undertaken towards the development of an analytical methodology to apply SERS directly to the painting surface. Minimally invasive SERS substrates have been proposed based on silver-doped methylcellulose removable gels specifically devised for use when investigating organic dyes and pigments in paint layers, providing an enhancement of Raman spectroscopy signals of about  $10^3$ – $10^4$  [102, 105, 106].

### 3.2 Non-invasive Identification of Binding Media and Other Polymers

Chromatographic techniques (such as gas chromatography mass spectrometry [GC–MS], pyrolysis gas chromatography mass spectrometry [Py–GC/MS], and HPLC) have been proven to be the most suitable and consolidated analytical methods for the full chemical characterization of natural and synthetic polymers (binders) in paint micro-samples. Often these analyses are profitably preceded by FTIR measurements on the same micro-samples, as a rapid method for a preliminary characterization of the polymers, with possible indications on the presence of pigments and fillers. In fact, binding media, basically proteins, glycosides, and lipids, in ancient art and a wide range of synthetic polymers in contemporary art show fairly distinctive vibrational features in the infrared range [107–110].

Non-invasive reflection FTIR spectroscopy has, therefore, significant diagnostic potentialities and, even in the presence of distortion effects due to the mixing of specular and diffuse reflection or overlaps by pigment absorption bands, it has been demonstrated to be a suitable technique for in situ discrimination of different families of binders, such as lipids, proteins, and alkyd, vinyl, or acrylic resins, without any sampling [12, 111].

#### 3.2.1 Preliminary Laboratory Tests

To facilitate diagnostics, detailed studies have been carried out on the most relevant features of near and mid-FTIR reflection spectra of binders in ancient and modern art [22, 24, 37, 111, 112]. The investigation was performed recording reflection spectra on paint reconstructions made of organic media (acrylic emulsion, polyvinyl acetate resin, alkyd resin, drying oil, and proteinaceous tempera) mixed with several pigments. This was done to better interpret any possible overlap of relevant vibrational absorption bands of pigments and binders in the region of interest of the spectra.

Spectral features relevant for diagnostics have been observed in three different regions of the infrared spectrum.

First, the so-called fingerprint region (between 2000 and 400  $\text{cm}^{-1}$ ) mainly containing the fundamental modes of binders, as the carbonyl stretching mode (1740–1730  $\text{cm}^{-1}$ ), the amide I, II and III bands (1680–1200  $\text{cm}^{-1}$ ), the CH bending modes (1380–1480  $\text{cm}^{-1}$ ), the symmetric stretching C–O–C mode (1300–1200  $\text{cm}^{-1}$ ), and the C–O and C–C stretching modes and C=C deformations (1200–700  $\text{cm}^{-1}$ ).

Second, the range between 3500 and 2800  $\text{cm}^{-1}$  that includes the CH and NH stretching modes of the organic binders. In particular, this range can be relevant for the detection of proteinaceous media thanks to the amide A (at ca. 3300  $\text{cm}^{-1}$ ) and amide B (at ca. 3070  $\text{cm}^{-1}$ ) bands [113] which, although not always visible, are quite characteristic of polypeptide structures.

Third, the portion of the spectrum between 6000 and 3900  $\text{cm}^{-1}$  corresponding to the near infrared, mainly including combination and overtone bands of organic compounds (CH, C=O, NH, C–O functional groups).

It has been noted that in the fingerprint region, vinyl and acrylic spectra show derivative-shaped profiles, while proteins and oils, and to a lesser extent alkyds, feature more broad bands (still distorted with respect to the transmission mode spectra). Thus, it can be inferred that for vinyl and acrylic films, the surface reflection is dominant while for the others there is a substantial contribution of volume reflection, the difference being most probably related to the different absorption coefficient of the polymers influencing the degree of light penetration. Diversely, the other two regions at higher wavenumbers are characterized by a prevalence of diffuse reflection. Generally, the presence of a pigment has the effect of increasing the contribution from volume reflection with a moderate broadening of the derivative shape that is stronger for the bands positioned at higher wavenumbers. Due to the possible coexistence of specular reflection and diffuse reflection, it is not advisable to transform the reflectance spectra via the Kramers–Kronig algorithm.

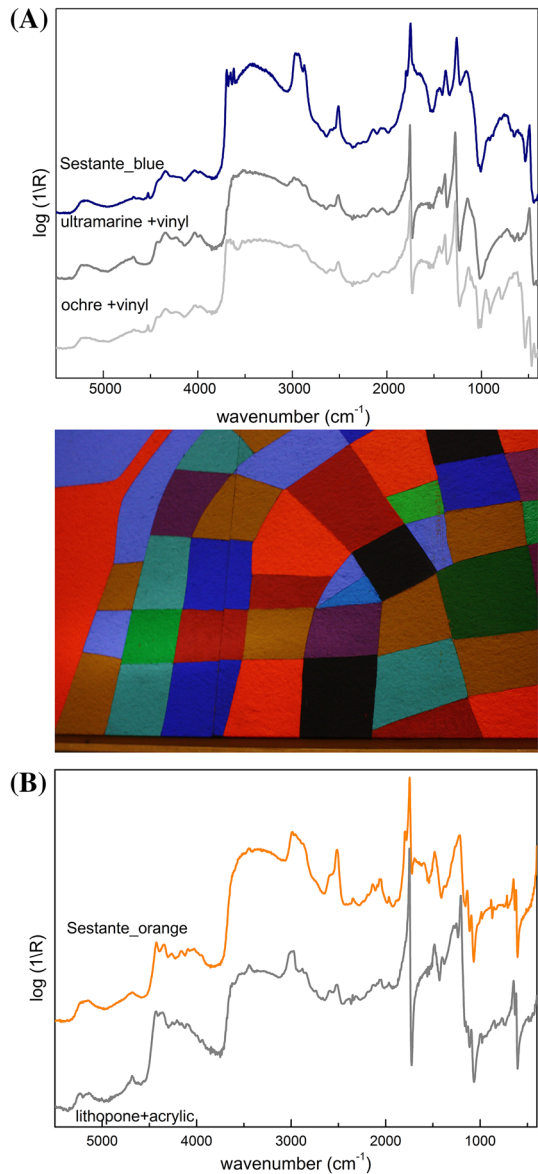
When all these features are taken into account, in spite of the spectral distortions arising from the sum of the specular and diffuse reflection related to the pigment-binder mixture and the overlaps with pigment bands, it is possible to individuate diagnostic bands for each polymeric compound that can be exploited for its non-invasive identification directly on ancient and modern paintings.

### 3.2.2 Examples of In Situ Studies

An initial example of the MOLAB analytical campaign is Memling's triptych, as presented in Fig. 1. In this case, the near-FTIR investigations registered C–H combination bands at 4260  $\text{cm}^{-1}$  ( $\nu_s\text{CH} + \delta\text{CH}$ ) and 4340  $\text{cm}^{-1}$  ( $\nu_a\text{CH} + \delta\text{CH}$ ), attributable to lipids [37], on all of the points measured on the three panels. The presence of lipids pointed towards the use of a drying oil and/or egg yolk as a binding medium. Weak protein signals (4595  $\text{cm}^{-1}$ , first overtone  $\nu\text{CO}$  amide I + amide II; 4880  $\text{cm}^{-1}$ , ( $\nu + \delta$ )NH) [37] were exclusively registered in some small, damaged paint areas, where the inner ground layer emerged, probably bound by glue [80].

A further example is within the study of the painting *Sestante 10* by Alberto Burri, a modern painting which is part of a series created by the artist in 1982, characterized by geometrical figures of different colour, shape, and surface roughness (Fig. 7). Here, the use of different binders in different figures was found. As shown in Fig. 7a, the spectrum recorded from a blue area showed features clearly attributable to a vinyl binder, with the contribution of both diffuse and

**Fig. 7** Detail of the painting *Sestante 10* by A. Burri. **a** reflection FTIR spectrum recorded in the indicated *blue area*. **b** reflection FTIR spectrum recorded on the indicated *red area* (see text)



specular reflected light, leading to a mixed derivative/positive shape. In addition, the comparison with reference models of ultramarine blue and ochre in a vinyl medium, together with other standard reference spectra for fillers (see Fig. 7a), allowed the presence of compounds, such as gypsum, calcium carbonate and kaolin to be detected. Diversely, the spectrum of Fig. 7b, recorded in a red area, perfectly fitted the reference spectrum from a standard of acrylic binder and lithopone, also reported in the figure. The similarity of the spectral profiles included the presence of the carbonyl band at about  $1740\text{ cm}^{-1}$ , the weaker CH bending at about  $1460\text{ cm}^{-1}$  and the acrylic marker band  $\nu(\text{CC})$  with inflection point around  $1175\text{ cm}^{-1}$ .

The exploitation of a large database of reference spectra for the interpretation of the relevant infrared reflection features recorded on paintings of several contemporary artists led very recently to the in situ characterisation of binding media in masterpieces by Hartung, Capogrossi, Turcato, Afro and other twentieth-century Italian artists [111].

## 4 New Perspectives: In Situ Chemical Imaging

The recent development of advanced methods for element-selective or species-selective imaging of painted surfaces has opened new perspectives for the non-invasive in situ study of paintings. In fact, through these methods, the distribution of elements or molecular moieties all over the entire painting can be drawn, giving relevant information on composition and distribution of materials at the surface and sub-surface of the paint. The information obtained profitably integrates the data by point analyses, significantly improving the understanding of the artist's creative process (in some cases, including the identification of underpaintings).

Imaging methods for the study of elemental and molecular distributions on the microscale are currently available in scanning electron microscopes or IR and Raman micro-spectrometers or at specific micro-analysis synchrotron beam lines. The extension of these imaging techniques to the macroscopic scale (large surface of several square centimetres) for in situ non-invasive studies is not straightforward and different approaches have been put recently into practice, each one with appropriate advantages and limitations. Some of these methods are full-field imaging methods, employing cameras or image plates sensitive to the range of the electromagnetic spectrum of interest, while others are based on a scanning-mode approach, using well-collimated beams over the painting.

### 4.1 X-ray Fluorescence Imaging

A scanner for macroscopic X-ray fluorescence imaging has been recently implemented by Alfeld et al. [114] at Antwerp University to determine the distribution of pigments on paintings over large areas. Although scanning conditions can be varied, the scanner consists of an XZ motor stage in a typical setup, covering a surface of  $60 \times 25\text{ cm}^2$ , on which a 10-W Rh anode transmission tube is mounted, together with a set of energy dispersive XRF detectors. In the scanning process, a typical 0.8-mm lead pinhole collimator is employed as a beam-defining optic,

yielding a beam size of ca. 1.2 mm at the surface of the paint. The scanning is carried out with a variable step size of 0.5–1 mm, with a variable dwell time.

Another macro-XRF scanner has become commercially available in recent years from Bruker Nano GmbH (Berlin, Germany) under the name M6-Jetstream. This system consists of an X-ray tube mounted with a silicon-drift-detector on an XZ motor stage. Through scanning, the distribution image of the main elements that compose the surface and sub-surface paint layers in an area of  $80 \times 60 \text{ cm}^2$  is obtained. The primary beam size can be varied between  $50 \text{ }\mu\text{m}$  and 1 mm, although high-resolution scans are only possible in areas of limited size [115].

Alfeld et al. [115] have employed the Antwerp prototype and tested the Bruker M6-Jetstream to carry out measurements on artworks of several painters. In particular, with the Antwerp macro-XRF scanner, several paintings by van Gogh, Goya, Memling, Rembrandt, amongst others [116, 117], have been investigated.

Due to the penetrative character of X-rays, the results obtained have been profitably exploited, not simply to draw the distribution of elements (and related pigments) over the surface, but also to reveal distinct features of underpaintings. In fact, when pigments used in underpaintings have a fairly different atomic composition with respect to those at the surface, the plot of the distribution of specific elements leads to underpaint images that emerge with a better clarity than achievable by traditional radiographies or IR reflectographies. In studies of works by Van Gogh [118], Goya [119] and Rembrandt [120, 121], paintings that were erroneously believed to be lost were found below the visible surface.

## 4.2 Hyperspectral infrared imaging

Delaney et al. have recently described the use of high-sensitivity, portable hyperspectral cameras suitable for the examination of paintings, drawings, and manuscripts' illuminations. These cameras can operate in various wavelength ranges, in the visible and near-IR (up to 2500 nm), and are characterized by high spectral (2.4–4 nm) and spatial resolutions (0.2–0.1 mm/pixel) [122–126].

These visible and near-infrared imaging spectroscopy systems have been exploited to identify and display the distribution of various pigments, utilizing electronic transitions, vibrational combination/overtone modes, and near-infrared luminescence. By this method, through in situ measurements, the pigments used by Picasso in the *Harlequin Musician* (1924), [122] part of the collection of the National Gallery of Art, Washington D.C., were identified and mapped. The results took significant advantage by the extension of imaging reflection spectroscopy up to 2500 nm and by the inclusion of luminescence imaging spectroscopy data. In addition, the combination with site-specific in situ analysis, such as XRF, strongly supported the achievement of a robust pigment identification and their mapping.

Very recently, the coupling of macro-XRF scanning and hyperspectral NIR imaging have been also attempted, showing the high potentiality of integrating the two imaging approaches to identify and map artist materials in an early Italian Renaissance panel painting [127].

In addition to the study of pigments, hyperspectral imaging in the near IR range has been also experimented to test the performance of the method for the study of



binders. The possible identification of these organic materials and their distribution throughout the painted surface has been demonstrated, exploiting the combinations and higher harmonics of the fundamental bands typical of the fingerprint mid-IR region which fall within the near-IR range. These chemical signatures include bands associated with CH, OH, NH and carbonyl groups. The method has been shown to be suitable for the mapping of egg yolk as binder in an early fifteenth-century illuminated manuscript attributed to Lorenzo Monaco [124] and the selective use of animal glue and egg yolk in a Cosme' Tura painting, dated 1475 (Fig. 8) [125, 127].

A recent work opened promising perspectives also towards the exploitation of hyperspectral imaging in the mid-IR range. A novel hyperspectral imager (model HI90, Bruker Optics, Portland, OR, USA), originally developed for the remote identification and localization of pollutants in the atmosphere, [128] was adapted for hyperspectral imaging of paintings, and used for identification and mapping of binding media on the painting *Sestante 10* (1982) by Alberto Burri already mentioned in Sect. 3.2 (see Fig. 7) [129]. The system, based on a focal plane array mercury–cadmium–telluride (MCT) detector with  $256 \times 256$  pixels, operates in the range  $900\text{--}1300\text{ cm}^{-1}$ , permitting the recording of mid-IR spectra to be carried out at each pixel, with  $4\text{-cm}^{-1}$  resolution. The system couples the focal plane array

**Fig. 8** Visible image and chemical map for Gabriel panel of Cosme' Tura's *The Annunciation with Saint Francis and Saint Louis of Toulouse* (Samuel H. Kress Collection, 1952.2.6, National Gallery of Art, Washington D.C.). *Left* Colour image. *Right* False-colour image showing the locations of binding media. Egg yolk binder (*red*) maps mainly to Gabriel's red robe. Glue binder (*blue*) maps to areas of the face and feet. Azurite in a glue binder (*green*) and malachite in an egg yolk binder (*yellow*) map to the sky and *dark green* tunic and wings, respectively. Reproduced from [125] with permission from The Royal Society of Chemistry



detector with an interferometer and, exploiting the multiplex advantage, allows for recording a complete hyperspectral data cube in one single measurement of a few tens of seconds.

With a setup based on  $128 \times 128$  pixels, three areas (ca.  $9 \times 9 \text{ cm}^2$ ) of the large painting ( $250 \times 360 \text{ cm}^2$ ) were analyzed on site at the Ex-Seccatoi del Tabacco (Citta' di Castello, Italy), where the painting is in permanent exhibition, through measurements that required 80 s per each cube.

Within the same areas explored by the HI90, point-analysis measurements have been also carried out with a portable FTIR spectrometer (Alpha-R, Bruker Optics, Portland, OR, USA) with the aim to validate the assignment made on the basis of the spectral data recorded at each pixel. These measurements revealed the excellent quality of the spectra collected by the hyperspectral imaging system, since the HI90 brightness temperature profiles recorded at each pixel were comparable to the corresponding Alpha-R reflection spectra (Fig. 9a, b).

The selective use by Burri of different binders to paint different areas of the *Sestante 10* cellotex panel was clearly put in evidence. In Fig. 9a, the visible image of a  $9 \times 9 \text{ cm}^2$  detail of *Sestante 10* is shown. The brightness temperature (BT) difference image, reported in Fig. 9b, shows the distribution of an acrylic binder in the red–orange sector, while the BT difference image shown in Fig. 9c, indicates the use of a vinyl binder common to the red, ochre, blue, cyan, and purple coloured areas.

Exploring the potentiality of spectroscopically imaging the mid-IR range, Legrand et al. [130] tested advantages and limitations of a prototype macroscopic mid-FTIR scanner. The scanning system consisted of a Bruker Alpha FTIR

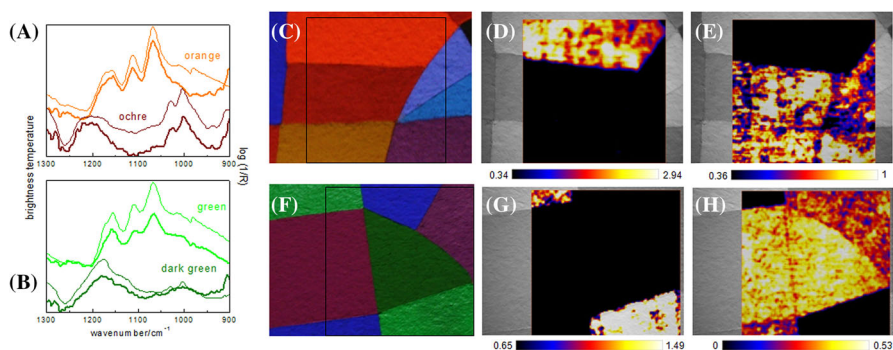


**Fig. 9** a, b Comparison of the spectral profiles recorded with the HI90 (*thick lines*) and the ALPHA-R spectrometer (*thin lines*) for the *orange*, *ochre*, *green* and *dark green* sectors of the painting *Sestante 10* by A. Burri (the *rectangles* highlight the spectral range considered for the chemical mapping). c, f Images of two details of the painting. The *black rectangle* highlights the areas investigated with the HI90 system (ca.  $9 \times 9 \text{ cm}^2$ ). d, g False-colour representations of the difference in the mean brightness temperature between  $1154$  and  $1167 \text{ cm}^{-1}$  and the mean brightness temperature between  $1197$  and  $1209 \text{ cm}^{-1}$  representing the acrylic medium distribution. e, h False-colour representation of the difference in the mean brightness temperature (measured in Kelvin) between  $1250$  and  $1255 \text{ cm}^{-1}$  and the mean brightness temperature between  $1220$  and  $1230 \text{ cm}^{-1}$ , representing the vinyl binder distribution (rearrangement from [129])

spectrometer that was moved all along the XZ plane in front of the painting, while FTIR spectra were recorded in reflection mode. Since this device scans the object point-by-point, the recording of full spectra over an extended mid-IR-range (7500–400  $\text{cm}^{-1}$ ) at each position is possible, identifying the compounds present and visualizing their distribution based on their fingerprint features. In one of the performance tests of the system, spectra were recorded on a detail ( $8 \times 8 \text{ cm}^2$ ) of an unvarnished folk-art panel painting of Antillean origin (probably twentieth century). The obtained mid-FTIR chemical distributions were compared and integrated with the elemental distributions recorded from macroscopic XRF imaging measurements on the same area, finding good correlations. The crossing of the data by the two approaches allowed a wide and satisfying visualization of pigment distributions in red, orange, yellow, green, and blue areas [130].

A comparison between the performances of the two full-field and macro-scanning approaches in mid-FTIR reveal complementary limits and potentials.

A substantial advantage of the macro-FTIR scanning configuration is that full spectra are recorded at each position all over the surface of the painting in the whole range from 7500 to 400  $\text{cm}^{-1}$ , obtaining a large quantity of exploitable data. However, a major important limitation of the prototype macro-FTIR scanner is the time required to record a hyperspectral dataset that can amount to numerous days for large surfaces. Nevertheless, many possibilities are available to improve this aspect, including the use of a more powerful source of mid-IR radiation and of larger beam focusing and/or collection optics for the reflected radiation. A great advantage of the full-field configuration of the Bruker HI90 is the fact that the time necessary to record all the spectra in the examined  $9 \times 9 \text{ cm}^2$  areas (16,384 spectra) amounts only to 80 s. A major limitation of the HI90 instrument is in the short wavenumber range that can be explored in the present configuration. This limit is expected to be overcome in the future with extension to larger wavenumber ranges.

An additional significant limitation of mid-IR imaging, in both full-field and macro-scanning approaches, lays in the fact that it can be significantly applied only to unvarnished paintings or to paintings where the varnish has been removed. Fortunately, for many paintings under restoration, the varnish is at least partially removed in the preliminary phases of the intervention.

All the innovative data acquired in the most recent years on macroscopic chemical imaging by XRF and near- and mid-IR spectroscopy open new significant perspectives for the in situ non-invasive study of paintings. In particular, in situ macro-XRF imaging is expected to become a widely diffused technique in the near future, due to both the availability of commercial instrumentation and the straightforward and reliable interpretation of elemental spectra. On the other side, both near and mid-IR imaging represent powerful techniques that can deliver complementary information on the distribution of inorganic and organic materials which cannot be detected or identified in a unique manner by means of XRF elemental data. In particular, they can give information on natural and synthetic binders otherwise impossible to be non-invasively mapped.

Further related research is currently in development for the setup of new methods for the in situ identification and mapping of chemical components on large areas of paintings. Of great interest are those regarding macro-XRD imaging, where

laboratory experiments based on application of synchrotron radiation sources lead to encouraging successful results [131, 132]. Using synchrotron light, high-energy (80–120 keV) XRD imaging has been recently experimented for the non-invasive measurement (in transmission mode) of crystalline phase distributions in paintings. Potentials and limitations of the experimented technique have been demonstrated using an authentic sixteenth-century painting as well as model paintings [132]. Very recently, promising preliminary experimentations have been carried out for the transfer of the technique from the synchrotron to a compact prototypical system suitable for in situ applications [117].

## 5 Conclusions

The results on the most recent in situ application of non-invasive methodologies outlined in this paper clearly show how the integration of data from different analytical techniques can successfully overcome the intrinsic limitation of each single spectroscopic method when applied on heterogeneous samples. At the same time, an accurate and systematic preliminary work on test samples allows for overcoming complications imposed by specific optical and matrix effects, making a satisfactory interpretation of reflection spectra possible.

The presented *modus operandi*, optimized after years of technological advances and experience, is based on exploring the atomic and the molecular levels, probing either electronic or vibrational properties (inducing absorption, emission and/or scattering phenomena), and employing techniques that are sensitive to highly or poorly ordered systems. The method allows today's researchers to successfully identify pigments in paintings with adequate certainty and completeness, fully avoiding sampling. In addition, through the exploitation of reflection near- and mid-FTIR spectroscopy, the family of natural binders widely used in ancient art (lipidic, proteic, glucosidic) can be disclosed, as well as of synthetic resins, as vinyl, acrylic, and alkyd, largely employed in contemporary art. Recently, thanks to accurate and detailed preliminary laboratory tests on a wide set of pigment specimens it has also become possible in some cases to distinguish composition and structures among a variety of inorganic pigments belonging to an extended series of compounds sharing the same chemical class, such as the series of chromate–sulfate coprecipitates, cadmium sulfides and lead antimonates. In this case, appropriate information is obtained by Raman spectroscopy through measurements that do not require long accumulation times nor specific arrangements, apart from control of the power of the radiation used. The unique advantage of Raman spectroscopy is the possibility to identify partial or totally amorphous phases frequently encountered in cases of pigments synthesized in ancient times.

More challenging is the identification of organic pigments. In this case, however, the synergic use of techniques such as FTIR, UV–Vis and Raman spectroscopy can lead to satisfactory results. In particular, while UV–Vis absorption and fluorescence can indicate a colorant's family, Raman spectroscopy can directly lead, in case of good scattering cross sections, to its unambiguous molecular identification. Interesting perspectives are opened by the rapid affirmation of SERS techniques,

although this approach for non-invasive in situ applications still remains at the experimental level.

Significant advances in the non-invasive in situ study of painting materials is represented by the chemical imaging techniques. A prototype macro-XRF scanner has been set up and exploited to identify and map the distribution of elements (and related pigments) over the surface of numerous paintings, as well as to reveal distinct features of underpaintings, with a clearness obtained better than that obtained by other traditional imaging techniques. By this method, paintings originally believed to be lost were brought to new light.

The most significant perspectives of further advancements rely on the infrared hyperspectral imaging. In the near-IR, the most recent hardware and software achievements allowed successful results to be obtained. A few cases of integrating macro-XRF and hyperspectral near-IR imaging have been also successfully experimented.

However, much work remains to be done for the development of methods in the mid-IR where the systems experimented to date have shown interesting solutions, but with problems still existing for data acquisition times, for the systems based on surface scanning, for extension of the explorable wavelength range, and for the full-field systems. In both cases, good perspectives for improvement are open, which rely on the use of a more powerful source of mid-IR radiation and better focusing and collection optics for the reflected radiation in case of the scanning method and on the introduction of new detectors for the full-field approach.

**Acknowledgments** The MOLAB activities described in this work were possible thanks to the support of the European Commission, through the Research Infrastructure projects Eu-ARTECH (FP6-RII3-CT-2004-506171) and CHARISMA (FP7-GA n. 228330) and of the Laboratorio di Diagnostica di Spoleto. The authors are grateful to several researchers that contributed to MOLAB activities: C. Anselmi, D. Buti, L. Cartechini, A. Chieli, A. Daveri, F. Gabrieli, C. Grazia, P. Moretti, F. Presciutti, M. Vagnini. Kind permission from J. Wiley and Sons to reproduce Fig. 5 (from Ref. [61]) and rearrange Fig. 9 (from Ref. [129]) is acknowledged. Figures 2, 3 and 4 are reproduced from Ref. [80] and Fig. 8 from Ref. [125] with permission of the Royal Society of Chemistry.

## References

1. Brunetti BG, Clark AJ, Sgamellotti A (eds) (2010) Advanced techniques in art conservation. *Acc Chem Res* 43(6):693-4
2. Sgamellotti A, Brunetti BG, Miliani C (eds) (2014) Science and art. The painted surface. The Royal Society of Chemistry, Cambridge
3. Clark RJH (1995) Raman microscopy: application to the identification of pigments on medieval manuscripts. *Chem Soc Rev* 24:187-196
4. Burgio L, Ciomartan DA, Clark RJH (1997) Pigment identification on medieval manuscripts, paintings and other artefacts by Raman microscopy: applications to the study of three German manuscripts. *J Mol Struct* 405:1-11
5. MacArthur JD, Del Carmine P, Lucarelli F, Mandò PA (1990) Identification of pigments in some colours on miniatures from the medieval age and early Renaissance. *Nucl Instr Meth B* 45:315-321
6. Wagner W, Neelmeijer C (1995) External proton beam analysis of layered objects. *Fresenius J Anal Chem* 353:297-302
7. Brissaud I, Guilló A, Lagarde G, Midya P, Calligaro T, Salomon J (1999) Determination of the sequence and thicknesses of multilayers in an easel painting. *Nucl Instr Meth B* 155:447-452

8. Janssens K, Vittiglio G, Deraedt I, Aerts A, Vekemans B et al (2000) Use of microscopic XRF for non-destructive analysis in art and archaeometry. *X-Ray Spectrom* 29:73–91
9. Eu-ARTECH, Access, research and technology for the conservation of the European Cultural Heritage, 6th FP RII3-CT-2004-506171 (2004–2009). [www.euartech.org](http://www.euartech.org)
10. CHARISMA, Cultural heritage advanced research infrastructures: synergy for a multidisciplinary approach to conservation, 7th FP GA n. 228330 (2009–2014). [www.charismaproject.eu](http://www.charismaproject.eu)
11. IPERION CH, Integrated platform for the European Research Infrastructure on Cultural Heritage, H2020 RIA n. 654028 (2014–2015). [www.iperionch.eu](http://www.iperionch.eu)
12. Miliani C, Rosi F, Brunetti BG, Sgamellotti A (2010) In situ non-invasive study of artworks: The MOLAB multi-technique approach. *Acc Chem Res* 43:728–738
13. Cesareo R, Frazzoli FV, Mancini C, Sciuti S, Marabelli M, Mora P, Rotondi P, Urbani G (1972) Non-destructive analysis of chemical elements in paintings and enamels. *Archaeometry* 14:65–78
14. Hall ET, Schweizer F, Toller PA (1973) X-ray fluorescence analysis of museum objects: a new instrument. *Archaeometry* 15:53–78
15. Moiola P, Seccaroni C (2000) Analysis of art objects using a portable X-ray fluorescence spectrometer. *X-Ray Spectrom* 29:48–52
16. Brunetti BG, Seccaroni C, Sgamellotti A (eds) (2004) *The painting technique of Pietro Vannucci, called il Perugino*. Nardini, Firenze
17. Roy A, Spring M (eds) (2007) *Raphael's painting technique: working practice before Rome*. Nardini, Firenze
18. Menu M, Ravaud E (eds) (2009) *Andrea Mantegna painting technique*. Special issue of *Techne'*. C2RMF, Paris
19. de Viguerie L, Solé VA, Walter Ph (2009) Multilayers quantitative X-ray fluorescence analysis applied to easel paintings. *Anal Bioanal Chem* 395:2015–2020
20. Bonizzoni L, Galli A, Poldi G, Milazzo M (2007) In situ non-invasive EDXRF analysis to reconstruct stratigraphy and thickness of Renaissance pictorial multilayers. *X-Ray Spectrom* 36:55–61
21. del Viguerie L, Walter Ph, Laval E, Mottin B, Solé VA (2010) Revealing the sfumato technique of Leonardo da Vinci by X-Ray fluorescence spectroscopy. *Angew Chem Int Ed* 49:6125–6128
22. Miliani C, Rosi F, Borgia I, Benedetti P, Brunetti BG, Sgamellotti A (2007) Fiber-optic Fourier Transform mid-infrared reflectance spectroscopy: A suitable technique for in situ studies of mural paintings. *Appl Spectrosc* 61:293–299
23. Miliani C, Rosi F, Burnstock A, Brunetti BG, Sgamellotti A (2007) Non-invasive in situ investigations versus micro-sampling: a comparative study on a Renoir's painting. *Appl Phys A* 89:849–856
24. Rosi F, Daveri A, Miliani C, Verri G, Benedetti P, Piqué F, Brunetti BG, Sgamellotti A (2009) Non-invasive identification of organic materials in wall paintings by fiber optic reflectance infrared spectroscopy: a statistical multivariate approach. *Anal Bioanal Chem* 395:2097–2106
25. Rosi F, Burnstock A, Van den Berg KJ, Miliani C, Brunetti BG, Sgamellotti A (2009) A non-invasive XRF study supported by multivariate statistical analysis and reflectance FTIR to assess the composition of modern painting materials. *Spectrochim. Acta A* 71:1655–1662
26. Kahrim K, Daveri A, Rocchi P, de Cesare G, Cartechini L, Miliani C, Brunetti BG, Sgamellotti A (2009) The application of in situ mid-FTIR fibre-optic reflectance spectroscopy and GC–MS analysis to monitor and evaluate painting cleaning. *Spectrochim Acta A* 74:1182–1188
27. Rosi F, Daveri A, Doherty B, Nazzareni S, Brunetti BG, Sgamellotti A, Miliani C (2010) On the use of overtone and combination bands for the analysis of the  $\text{CaSO}_4\text{-H}_2\text{O}$  system by mid-infrared reflection spectroscopy. *Appl Spectrosc* 64:956–963
28. Miliani C, Rosi F, Daveri A, Brunetti BG (2012) Reflection infrared spectroscopy for the non-invasive in situ study of artists' pigments. *Appl Phys A* 106:295–307
29. Buti D, Rosi F, Brunetti BG, Miliani C (2013) In-situ identification of copper-based green pigments. *Anal Bioanal Chem* 405:2699–2711
30. Doherty B, Daveri A, Clementi C, Romani A, Bioletti S, Brunetti BG, Sgamellotti A, Miliani C (2013) The Book of Kells: A non-invasive MOLAB investigation by complementary spectroscopic techniques. *Spectrochim Acta A* 115:330–336
31. Daveri A, Doherty B, Moretti P, Grazia C, Romani A, Fiorin E, Brunetti BG, Vagnini M (2015) An uncovered XIII century icon: Particular use of organic pigments and gilding techniques highlighted by analytical methods. *Spectrochim Acta A* 135:398–404

32. Buti D, Domenici D, Miliani C, García Sáiz C, Gómez Espinoza T, Jiménez Villalba F, Verde Casanova A, Sabiá de la Mata A, Romani A, Presciutti F, Doherty B, Brunetti BG, Sgamellotti A (2014) Non-invasive investigation of a pre-Hispanic Maya screenfold book: The Madrid Codex. *J Archaeol Sci* 42:166–178
33. Fabbri M, Picollo M, Porcinai S, Bacci M (2001) Mid-infrared fiber-optics reflectance spectroscopy: A non-invasive technique for remote analysis of painted layers. Part I: Technical setup. *Appl Spectrosc* 55:420–427
34. Fabbri M, Picollo M, Porcinai S, Bacci M (2001) Mid-infrared fiber-optics reflectance spectroscopy: A non-invasive technique for remote analysis of painted layers. Part II: Statistical analysis of spectra. *Appl Spectrosc* 55:428–433
35. Griffiths P, De Haseth JA (2007) *Fourier transform infrared spectrometry*, 2nd edn. Wiley, New York
36. Miliani C, Daveri A, Brunetti BG, Sgamellotti A (2008) CO<sub>2</sub> entrapment in natural ultramarine blue. *Chem Phys Lett* 446:148–151
37. Vagnini M, Miliani C, Cartechini L, Rocchi P, Brunetti BG, Sgamellotti A (2009) FT-NIR spectroscopy for non-invasive identification of natural polymers and resins in easel paintings. *Anal Bioanal Chem* 395:2107–2118
38. Jurado Lopez A, Luque De Castro MD (2004) Use of near-infrared spectroscopy in a study of binding media in paintings. *Anal Bioanal Chem* 380:706–771
39. Wendlandt WW, Hecht HG (1966) *Reflectance spectroscopy*. Interscience Publishers, New York
40. Bacci M, Baldini F, Carlá R, Linari R, Picollo M, Radicati B (1993) Colour analysis of the Brancacci Chapel frescoes. *Appl Spectrosc* 47:399–402
41. Bacci M, Casini A, Cucci C, Picollo M, Radicati B, Vervat M (2003) Non-invasive spectroscopic measurements on the “Il ritratto della figliastra” by Giovanni Fattori: identification of pigments and colorimetric analysis. *J Cult Herit* 4:329–336
42. Bacci M, Picollo M, Trumpy G, Tsukada M, Kunzelman D (2007) Non-invasive identification of white pigments on 20th-century oil paintings by using fiber optic reflectance spectroscopy. *J Am Inst Conserv* 46:27–37
43. Bruni S, Caglio S, Guglielmi V, Poldi G (2008) The joined use of non-invasive spectroscopic analyses – FTIR, Raman, visible reflectance spectrometry and EDXRF – to study drawings and illuminated manuscripts. *Appl Phys A* 92:103–108
44. Ricciardi P, Delaney J, Facini M, Glinsman L (2013) Use of imaging spectroscopy and in situ analytical methods for the characterization of the materials and techniques of 15th century illuminated manuscripts. *J Am Inst Conserv* 52:13–29
45. Aceto M, Agostino A, Fenoglio G, Idone A, Gulmini M, Picollo M, Ricciardi P, Delaney JK (2014) Characterisation of colourants on illuminated manuscripts by portable fibre optic UV–visible-NIR reflectance spectrophotometry. *Anal Methods* 6:1488–1500
46. Romani A, Clementi C, Miliani C, Favaro G (2010) Fluorescence Spectroscopy: A Powerful Technique for the Noninvasive Characterization of Artwork. *Acc Chem Res* 43:837–846
47. Clementi C, Doherty B, Gentili P, Miliani C, Romani A, Brunetti BG, Sgamellotti A (2008) Vibrational and electronic properties of painting lakes. *Appl Phys A* 92:25–33
48. Clementi C, Miliani C, Romani A, Favaro G (2006) In situ fluorimetry: A powerful noninvasive diagnostic technique for natural dyes used in artefacts Part I. Spectral characterization of orcein in solution, on silk and wool laboratory-standards and a fragment of Renaissance tapestry. *Spectrochim Acta, Part A* 64:906–912
49. Miliani C, Romani A, Favaro G (1998) Spectrophotometric and fluorimetric study of some anthraquinoid and indigoid colorants used in artistic paintings. *Spectrochim Acta, Part A* 54:581–588
50. Buti D (2009) Ph.D. Thesis, University of Firenze
51. Clementi C, Rosi F, Romani A, Vivani R, Brunetti BG, Miliani C (2012) Photoluminescence properties of zinc oxide in paints: A study of the effect of self-absorption and passivation. *Appl Spectrosc* 66:1233–1241
52. Rosi F, Grazia C, Gabrieli F, Romani A, Paolantoni M, Vivani R, Brunetti BG, Colombari Ph, Miliani C (2016) UV–Vis-NIR and micro Raman spectroscopies for the non destructive identification of Cd<sub>1-x</sub>Zn<sub>x</sub>S solid solutions in cadmium yellow pigments. *Microchem J* 124:856–867
53. Grazia C, Rosi F, Gabrieli F, Romani A, Paolantoni M, Vivani R, Brunetti BG, Colombari Ph, Miliani C (2016) A multitechnique approach for investigating the composition of ternary CdS<sub>1-x</sub>Se<sub>x</sub> solid solutions employed as artists’ pigments. *Microchem J* 125:279–289

54. Accorsi G, Verri G, Bolognesi M, Armaroli N, Clementi C, Miliani C, Romani A (2009) The exceptional near-infrared luminescence properties of cuprorivaite (Egyptian blue). *Chem Commun* 3392–3394
55. Clementi C, Miliani C, Verri G, Sotiropoulou S, Romani A, Brunetti BG, Sgamellotti A (2009) Application of the Kubelka-Munk correction for self-absorption of fluorescence emission in carmine lake paint layers. *Appl Spectrosc* 63:1323–1330
56. Simonot L, Thoury M, Delaney JK (2011) Extension of the Kubelka-Munk theory for fluorescent turbid media to a non-opaque layer on a background. *J Opt Soc Am* 28:1349–1357
57. Romani A, Clementi C, Miliani C, Brunetti BG, Sgamellotti A, Favaro G (2008) Portable equipment for luminescence lifetime measurements on surfaces. *Appl Spectrosc* 62:1395–1399
58. Nevin A, Cesaratto A, Bellei S, D'Andrea C, Toniolo L, Valentini G, Comelli D (2014) Time-Resolved Photoluminescence Spectroscopy and Imaging: New Approaches to the Analysis of Cultural Heritage and Its Degradation. *Sensors* 14:6338–6355 **and references therein**
59. Romani A, Grazia C, Anselmi C, Miliani C, Brunetti BG (2011) New portable instrument for combined reflectance, time-resolved and steady-state luminescence measurements on works of art. In: Pezzati L, Salimbeni R (eds) *SPIE Proceedings* Vol. 8084: O3A: Optics for Arts, Architecture, and Archaeology III. doi:10.1117/12.889529
60. Colomban Ph (2012) The on-site/remote Raman analysis with mobile instruments: a review of drawbacks and success in cultural heritage studies and other associated fields. *J Raman Spectrosc* 43:1529–1535
61. Monico L, Janssens K, Hendriks E, Brunetti BG, Miliani C (2014) Raman study of different crystalline forms of  $\text{PbCrO}_4$  and  $\text{PbCr}_{1-x}\text{S}_x\text{O}_4$  solid solutions for the non-invasive identification of chrome yellows in paintings: a focus on works by Vincent van Gogh. *J Raman Spectrosc* 45:1034–1045
62. Nakai I, Abe Y (2012) Portable X-ray powder diffractometer for the analysis of art and archaeological materials. *Appl Phys A* 106:279–293
63. Gatto Rotondo G, Romano FP, Pappalardo G, Pappalardo L, Rizzo F (2010) Nondestructive characterization of fifty various species of pigments of archaeological and artistic interest by using the portable X-ray diffraction system of the LANDIS laboratory of Catania (Italy). *Microchem J* 96:252–258
64. Romano FP, Pappalardo L, Masini N, Pappalardo G, Rizzo F (2011) The compositional and mineralogical analysis of fired pigments in Nasca pottery from Cahuachi (Peru') by the combined use of the portable PIXE-alpha and portable XRD techniques. *Microchem J* 99:449–453
65. Chiari G (2008) Saving art in situ. *Nature* 453:159
66. Sarrazin P, Chiari G, Gailhanou M (2008) A portable non-invasive XRF/XRD instrument for the study of art objects. *Adv X-Ray Anal* 52:175–186
67. Gianoncelli A, Castaing J, Ortega L, Dooryhée E, Salomon J, Walter Ph, Hodeau JL, Bordet P (2008) X-Ray Spectrom 37:418–423
68. Duran A, Perez-Rodriguez JL, Espejo T, Franquelo ML, Castaing J, Walter Ph (2009) *Anal Bioanal Chem* 395:1997–2004
69. Pages-Camagna S, Laval E, Vigears D, Duran A (2010) Non-destructive and in situ analysis of Egyptian wall paintings by X-ray diffraction and X-ray fluorescence portable systems. *Appl Phys A* 100:671–675
70. Chiari G (2010) Analyzing stratigraphy with a dual XRD/XRF instrument. Denver X-ray conference abstracts. [http://www.dxcicdd.com/10/DXC\\_list\\_abstract.asp](http://www.dxcicdd.com/10/DXC_list_abstract.asp)
71. Uda M, Ishizaki A, Satoh R, Okada K, Nakajima Y, Yamashita D, Ohashi K, Sakuraba Y, Shimono A, Kojima D (2005) Portable X-ray diffractometer equipped with XRF for archaeometry. *Nucl Instr Meth B* 239:77–84
72. Mendoza Cuevas A, Perez Gravie H (2011) Portable energy dispersive X-ray fluorescence and X-ray diffraction and radiography system for archaeometry. *Nucl Instrum Methods A* 633:72–78
73. Mendoza Cuevas A, Bernardini F, Gianoncelli A, Tuniz C (2015) Energy dispersive X-ray diffraction and fluorescence portable system for cultural heritage applications. *X-Ray Spectrom* 44:105–115
74. Bracci S, Falletti F, Matteini M, Scopigno R (eds) (2004) *Exploring David. Diagnostic tests and state of conservation*. Giunti, Firenze
75. Monico L, Janssens K, Miliani C, Brunetti BG, Vagnini M et al (2013) Degradation process of lead chromate in paintings by Vincent van Gogh studied by means of spectromicroscopic methods. 3.



- Synthesis, characterization, and detection of different crystal forms of the chrome yellow pigment. *Anal Chem* 85:851–859
76. Monico L, Janssens K, Hendricks E, Vanmeert F, Van der Schnickt G, Cotte M, Falkenberg G, Brunetti BG, Miliani C (2015) Evidence for degradation of the chrome yellows in Van Gogh Sunflowers: a study by non-invasive methods and synchrotron radiation-based X-ray techniques. *Angew Chem Int Ed* 54:13923–13927
  77. Casadio F, Miliani C, Rosi F, Romani A, Anselmi C, Brunetti BG, Sgamellotti A, Andral JL, Gautier G (2013) Scientific investigations on an important corpus of Picasso paintings in Antibes: New insights into technique, conditions and chronological sequence. *J Am Inst Conserv* 52:184–204
  78. Rosi F, Miliani C, Clementi C, Kahrim K, Presciutti F, Vagnini M, Manuali V, Daveri A, Cartechini L, Brunetti BG, Sgamellotti A (2010) An integrated spectroscopic approach for the non-invasive study of modern art materials and techniques. *Appl Phys A* 100:613–624
  79. Van Bommel MR, Janssen H, Spronk R (eds) (2012) *Inside out Victory Boogie Woogie. A material history of Mondrian's masterpiece.* Amsterdam University Press, Amsterdam
  80. Van der Snickt G, Miliani C, Janssens K, Brunetti BG, Romani A, Rosi F, Walter Ph, Castaing J, De Nolf W, Klaassen L, Labarque I, Wittermann R (2011) Material analyses of “Christ with singing and music-making angels”, a late 15th C panel painting attributed to Hans Memling and assistants: Part I. non-invasive in situ investigations. *J Anal At Spectrom* 26:2216–2229
  81. Ricci C, Miliani C, Brunetti BG, Sgamellotti A (2006) Non-invasive identification of surface materials on marble artifacts with fiber optic mid-FTIR reflectance spectroscopy. *Talanta* 61:1221–1226
  82. Gettens RJ, Mrose ME (1954) Calcium Sulphate Minerals in the Grounds of Italian Paintings. *Stud Conserv* 1:174–189
  83. Szmelter I, Cartechini L, Romani A, Pezzati L (2014) Multi-criterial studies of the masterpiece The Last Judgement, attributed to H. Memling, at the National Museum of Gdansk. In: Sgamellotti A, Brunetti BG, Miliani C (eds) *Science and art. The painted surface.* The Royal Society of Chemistry, Cambridge
  84. Hradil D, Grygar T, Hradilova J, Bezdicka P, Grunwaldova V, Fogas I, Miliani C (2007) Micro-analytical identification of Pb-Sb-Sn yellow pigment in historical European paintings and its differentiation from lead tin and Naples yellows. *J Cult Herit* 8:377–383
  85. Rosi F, Manuali V, Miliani C, Brunetti BG, Sgamellotti A, Grygar T, Hradil D (2009) Raman scattering features of lead pyroantimonate compounds. Part I: XRD and Raman characterization of Pb<sub>2</sub>Sb<sub>2</sub>O<sub>7</sub> doped with tin and zinc. *J Raman Spectrosc* 40:107–111
  86. Rosi F, Manuali V, Grygar T, Bezdicka P, Brunetti BG, Sgamellotti A, Burgio L, Seccaroni C, Miliani C (2011) Raman scattering features of lead pyroantimonate compounds: implication for the non-invasive identification of yellow pigments on ancient ceramics. Part II. In situ characterisation of Renaissance plates by portable micro-Raman and XRF studies. *J Raman Spectrosc* 42:407–414
  87. Cartechini L, Rosi F, Miliani C, D'Acapito F, Brunetti BG, Sgamellotti A (2011) Modified Naples yellow in Renaissance majolica: study of Pb–Sb–Zn and Pb–Sb–Fe ternary pyroantimonates by X-ray absorption spectroscopy. *J Anal At Spectrom* 26:2500–2507
  88. Fiedler I, Bayard MA (1986) Cadmium yellow orange and red. In: Feller RL (ed) *Artist's Pigments, a handbook of their history and characteristics, vol 1.* Cambridge University Press, Cambridge, pp 65–108
  89. Huckle WG, Swigert GF, Wiberley SE (1966) Cadmium Pigments. Structure and Composition. *Ind Eng Chem Prod Res Dev* 5:362–366
  90. Kirby J, Stonor K, Roy A, Burnstock A, Grout R, White R (2003) *Seurat's Painting Practice: Theory, Development and Technology.* Natl Gallery Tech Bull 24:4–37
  91. Van der Snickt G, Janssens K, Schalm O, Aibéo C, Klouft H, Alfeld M (2010) James Ensor's pigment use: artistic and material evolution studied by means of portable X-ray fluorescence spectrometry. *X-Ray Spectrom* 39:103–111
  92. Hendriks E (2006) In: Hendriks E, Van Tilborgh L (eds) *New Views on Van Gogh's development in Antwerp and Paris: an integrated art historical and technical study of his paintings in the Van Gogh Museum.* University of Amsterdam, Amsterdam, pp 149–150
  93. Kühn H, Curran M (1986) Chrome yellow and other chromate pigments. In: Feller RL (ed) *Artists' pigments: a handbook of their history and characteristics, vol 1.* Cambridge University Press, Cambridge, pp 187–200
  94. Eastaugh N, Walsh V, Chaplin T, Siddall R (2004) *The pigment compendium (CD-ROM).* Elsevier, Amsterdam

95. Monico L, Van der Snickt G, Janssens K, De Nolf W, Miliani C, Verbeeck J, Tian H, Tan H, Dik J, Radepont M, Cotte M (2011) Degradation process of lead chromate in paintings by Vincent van Gogh studied by means of synchrotron X-ray spectromicroscopy and related methods. 1. Artificially aged model samples. *Anal Chem* 83:1214–1223 **and references therein**
96. Monico L, Van der Snickt G, Janssens K, De Nolf W, Miliani C, Dik J, Radepont M, Hendriks E, Geldof M, Cotte M (2011) Degradation process of lead chromate in paintings by Vincent van Gogh studied by means of synchrotron X-ray spectromicroscopy and related methods. 2. Original paint layer samples. *Anal Chem* 83:1224–1231 **and references therein**
97. Monico L, Janssens K, Miliani C, Van der Snickt G, Brunetti BG, Cestelli Guidi M, Radepont M, Cotte M (2013) Degradation Process of Lead Chromate in Paintings by Vincent van Gogh Studied by Means of Spectromicroscopic Methods. 4. Artificial aging of model samples of co-precipitates of lead chromate and lead sulfate. *Anal Chem* 85:860–867
98. Monico L, Janssens K, Vanmeert F, Cotte M, Brunetti BG, Van der Snickt G, Leeuwestein M, Salvant Plisson J, Menu M, Miliani C (2014) Degradation process of lead chromate in paintings by Vincent van Gogh studied by means of spectromicroscopic methods. Part 5. Effects of non-original surface coatings into the nature and distribution of chromium and sulfur species in chrome yellow paints. *Anal Chem* 86:10804–10811
99. Monico L, Janssens K, Cotte M, Romani A, Sorace L, Grazia C, Brunetti BG, Miliani C (2015) Synchrotron-based X-ray spectromicroscopy and electron paramagnetic resonance spectroscopy to investigate the redox properties of lead chromate pigments under the effect of the visible light. *J Anal At Spectrosc* 30:2024
100. Herbst W, Hunger K (2004) Industrial organic pigments production, properties, applications. Wiley, New York
101. Van Bommel MR, Vanden Berghe I, Wallert AM, Boitelle R, Wouters J (2007) High-performance liquid chromatography and non-destructive three-dimensional fluorescence analysis of early synthetic dyes. *J Chromatogr A* 1120:260–272
102. Doherty B, Vagnini M, Dufourmantelle K, Sgamellotti A, Brunetti BG, Miliani C (2014) A vibrational spectroscopic and principal component analysis of triarylmethane dyes by comparative laboratory and portable instrumentation. *Spectrochim Acta A* 12:292–305
103. Sherrer NC, Stephan Z, Francoise D, Annette F, Renate K (2009) Synthetic organic pigments of the 20th and 21st century relevant to artist's paints: Raman spectra reference collection. *Spectrochim Acta A* 73:505–524
104. Vandenebe P, Moens L, Edwards HGM, Dams R (2000) Raman spectroscopic database of azo pigments and application to modern art studies. *J Raman Spectrosc* 31:509–517
105. Doherty B, Brunetti BG, Sgamellotti A, Miliani C (2011) A detachable SERS active cellulose film: a minimally invasive approach to the study of painting lakes. *J Raman Spectrosc* 42:1932–1938
106. Doherty B, Presciutti F, Sgamellotti A, Brunetti BG, Miliani C (2014) Monitoring of optimized SERS active gel substrates for painting and paper substrates by unilateral NMR profilometry. *J Raman Spectrosc* 45:1153–1159
107. Learner TJ (2004) Analysis of modern paints. Research in conservation. Getty Conservation Institute, Los Angeles
108. Cappitelli F, Learner T, Chiantore O (2002) An initial assessment of thermally assisted hydrolysis and methylation—gas chromatography/mass spectrometry for the identification of oils from dried paint films. *J Anal Appl Pyrolysis* 63:339–348
109. Silva MF, Doménech-Carbó MT, Fuster-Lopéz L, Martín-Rey S, Mecklenburg MF (2009) Determination of the plasticizer content in poly(vinyl acetate) paint medium by pyrolysis–silylation–gas chromatography–mass spectrometry. *J Anal Appl Pyrolysis* 85:487–491
110. Peris-Vicente J, Baumer U, Stege H, Lutzenberger K, Gimeno Adelantado JV (2009) Characterization of commercial synthetic resins by Pyrolysis-Gas Chromatography/Mass Spectrometry: Application to modern art and conservation. *Anal Chem* 81:3180–3187
111. Rosi F, Daveri A, Moretti P, Brunetti BG, Miliani C (2016) Interpretation of mid and near-infrared reflection properties of synthetic polymer paints for the non-invasive assessment of binding media in twentieth-century pictorial artworks. *Microchem J* 124:898–908
112. Ploeger R, Chiantore O, Scalzone D, Poli T (2011) Mid-infrared fiber-optic reflection spectroscopy analysis of artists' alkyd paints on different supports. *Appl Spectrosc A* 65:429–435
113. Barth A, Zscherp C (2002) What vibrations tell us about proteins. *Q Rev Biophys* 35:369–430

114. Alfeld M, Janssens K, Dik J, de Nolf W, van der Snickt G (2011) Optimization of mobile scanning macro-XRF systems for the in situ investigation of historical paintings. *J Anal At Spectrom* 26:899–909
115. Alfeld M, Pedroso JV, Hommes MV, van der Snickt G, Tauber G, Blaas J, Haschke M, Erler K, Dik J, Janssens K (2013) A mobile instrument for in situ scanning macro-XRF investigation of historical paintings. *J Anal At Spectrom* 28:760–776
116. Janssens K, Dik J, Cotte M, Susini J (2010) Photon-Based Techniques for Nondestructive Sub-surface Analysis of Painted Cultural Heritage Artifacts. *Acc Chem Res* 43:814–825
117. Legrand S, Vanmeert F, Van der Snickt G, Alfeld M, De Nolf W, Dik J, Janssens K (2014) Examination of historical paintings by state-of-the-art hyperspectral imaging methods: from scanning infra-red spectroscopy to computed X-ray laminography. *Herit Sci* 2:13 **and references therein**
118. Alfeld M, van der Snickt G, Vanmeert F, Janssens K, Dik J, Appel K, van der Loeff L, Chavannes M, Meedendorp T, Hendriks E (2013) Scanning XRF investigation of a Flower Still Life and its underlying composition from the collection of the Kroller-Muller Museum. *Appl Phys A* 111:165–175
119. Bull D, Krekeler A, Alfeld M, Dik J, Janssens K (2011) An intrusive portrait by Goya. *Burlingt Mag* 153:668–673
120. Alfeld M, De Nolf W, Cagno S, Appel K, Siddons DP, Kuczewski A, Janssens K, Dik J, Trentelman K, Walton M, Sartorius A (2013) Revealing hidden paint layers in oil paintings by means of scanning macro-XRF: a mock-up study based on Rembrandt's "An old man in military costume". *J Anal At Spectrom* 28:40–43
121. Trentelman K, Janssens K, van der Snickt G, Szafran Y, Woollett AT, Dik J (2015) Rembrandt's "An old man in military costume" the underlying image re-examined. *Appl Phys A*. doi:[10.1007/s00339-015-9426-3](https://doi.org/10.1007/s00339-015-9426-3)
122. Delaney JK, Zeibel JG, Thoury M, Littleton R, Palmer M, Morales KM, de la Rie ER, Hoenigswald A (2010) Visible and Infrared imaging spectroscopy of Picasso's Harlequin musician: mapping and identification of artist materials in situ. *Appl Spectrosc* 64:584–594
123. Thoury M, Delaney JK, de la Rie ER, Palmer M, Morales K, Krueger J (2011) Near-infrared luminescence of cadmium pigments: in situ identification and mapping in paintings. *Appl Spectrosc* 65:939–951
124. Ricciardi P, Delaney JK, Facini M, Zeibel JG, Picollo M, Lomax S, Loew M (2012) Near infrared reflectance imaging spectroscopy to map paint binders in situ on illuminated manuscripts. *Angew Chem Int Ed* 51:5607–5610
125. Dooley KA, Lomax S, Zeibel JG, Miliani C, Ricciardi P, Hoenigswald A, Loew M, Delaney JK (2013) Mapping of egg yolk and animal skin glue paint binders in Early Renaissance paintings using near infrared reflectance imaging spectroscopy. *Analyst* 138:4838–4848
126. Muir K, Langley A, Bezur A, Casadio F, Delaney JK, Gautier G (2012) Scientifically investigating Picasso's suspected use of Ripolin house paints in still life, 1922, and the red armchair, 1931. *J Am Inst Conserv* 52:156–172
127. Dooley KA, Conover DM, Deming Glinesman L, Delaney JK (2014) Complementary Standoff Chemical Imaging to Map and Identify Artist Materials in an Early Italian Renaissance Panel Painting. *Angew Chem Int Ed* 53:13775–13779
128. Sabbah S, Harig R, Rusch P, Eichmann J, Keens A, Gerhard J (2012) Remote sensing of gases by hyperspectral imaging: system performance and measurements. *Opt Eng* 51:111717
129. Rosi F, Miliani C, Braun R, Harig R, Sali D, Brunetti BG, Sgamellotti A (2013) Noninvasive analysis of paintings by mid-infrared hyperspectral imaging. *Angew Chem Int Ed* 52:5258–5261
130. Legrand S, Alfeld M, Vanmeert F, De Nolf W, Janssens K (2014) Macroscopic reflection Fourier Transformed Mid-Infrared (MA-rFTIR) scanning, a new technique for in situ imaging of painted cultural artefacts. *Analyst* 139:2489–2498
131. Doryhee F, Anne M, Bardies I, Hodeau JL, Martinetto P, Rondot S, Salomon J, Waughan GBM, Walter Ph (2005) Non-destructive synchrotron X-ray diffraction mapping of a Roman painting. *Appl Phys A* 81:663–667
132. De Nolf W, Dik J, Van der Snickt G, Wallert A, Janssens K (2011) High energy X-ray powder diffraction for the imaging of (hidden) paintings. *J Anal At Spectrom* 26:910–916